

Published in final edited form as:

Prog Part Nucl Phys. 2023 July ; 131: 104046. doi:10.1016/j.pnp.2023.104046.

## Emerging technologies for cancer therapy using accelerated particles

Christian Graeff<sup>a,b</sup>, Lennart Volz<sup>a</sup>, Marco Durante<sup>a,b,c,\*</sup>

<sup>a</sup>GSI Helmholtzzentrum für Schwerionenforschung, Biophysics Department, Planckstraße 1, 64291 Darmstadt, Germany

<sup>b</sup>Technische Universität Darmstadt, Darmstadt, Germany

<sup>c</sup>Dipartimento di Fisica “Ettore Pancini”, University Federico II, Naples, Italy

### Abstract

Cancer therapy with accelerated charged particles is one of the most valuable biomedical applications of nuclear physics. The technology has vastly evolved in the past 50 years, the number of clinical centers is exponentially growing, and recent clinical results support the physics and radiobiology rationale that particles should be less toxic and more effective than conventional X-rays for many cancer patients. Charged particles are also the most mature technology for clinical translation of ultra-high dose rate (FLASH) radiotherapy. However, the fraction of patients treated with accelerated particles is still very small and the therapy is only applied to a few solid cancer indications. The growth of particle therapy strongly depends on technological innovations aiming to make the therapy *cheaper, more conformal* and *faster*. The most promising solutions to reach these goals are superconductive magnets to build compact accelerators; gantryless beam delivery; online image-guidance and adaptive therapy with the support of machine learning algorithms; and high-intensity accelerators coupled to online imaging. Large international collaborations are needed to hasten the clinical translation of the research results.

### Keywords

Particle therapy; Medical accelerators; Gantry; FLASH; Moving targets; Radioactive ions

## 1 Introduction

For many millennia, infections and neonatal diseases have been the leading causes of human mortality worldwide. Only in the XXI century, cardiovascular diseases and cancer got the first positions [1], as already was the case in the industrialized countries since many years. The main risk factors for these diseases is age, i.e. they become prevalent when life

\*Corresponding author at: GSI Helmholtzzentrum für Schwerionenforschung, Biophysics Department, Planckstraße 1, 64291 Darmstadt, Germany. M.Durante@gsi.de (M. Durante).

#### Declaration of competing interest

The authors declare the following financial interests/personal relationships which may be considered as potential competing interests: Marco Durante reports financial support was provided by European Union.

expectancy increase. Cancer is the 2nd most common cause of death worldwide and cancer therapy is therefore obviously in the forefront of medical research [2,3]. Even if enormous progress in systemic pharmacological approaches have been accomplished recently, local therapies – surgery and radiotherapy – remain indispensable. Radiotherapy is indeed used for over 50% of the cancer patients, sometimes as single treatment option but more often as a part of the multimodal cancer care.

The ultimate goal of curative radiotherapy is to kill the tumor cells with acceptable toxicity for the surrounding normal tissues. The effectiveness in killing malignant and normal cells primarily depends on the ionizing radiation dose i.e. the energy deposited per unit target mass (measured in gray; 1 Gy = 1 J/kg). Every tumor can be destroyed if the dose is high enough, but the prescribed dose is limited by the normal tissues surrounding the malignancy. Treatments of malignancies with radiation started only months after the discovery of X-rays by Wilhelm Röntgen in 1895, and in over a century of technological progress underwent many modifications and increasing complexity and automation [4,5]. Currently over 80% of the patients eligible for radiotherapy are treated with external beams (teletherapy) of X-rays produced by bremsstrahlung of electrons accelerated in linacs to about 6 MeV. The others are treated with specialized treatments such as gamma knife or brachytherapy, and less than 1% is treated with accelerated charged particles (protons or heavier ions) [6]. This number is, however, steadily increasing [7].

According to the Particle Therapy Co-Operative Group (PTCOG) database [8], 324.586 patients were treated with charged particles until the end of 2021. Around 86% of those patients were treated with protons. The number of facilities in operation is also rapidly increasing in the past years (Fig. 1) [9]. Whilst most of the facilities are in Japan and in the USA, many other countries are in rapid expansion such as Spain (11 centers are planned in addition to the two in operation in Madrid) or China [10].

The rationale for particle therapy lies in its physical properties. Unlike X-rays, the energy deposited per unit track length increases with depth (Fig. 2), therefore for a single beam the dose to the normal tissue will be much lower for ions than for photons when delivering the same dose to the tumor. Particle therapy is therefore intrinsically more *conformal* than X-ray therapy, i.e. can provide excellent high dose distributions in tumors of complex shape with relatively low dose to the surrounding normal tissue (Fig. 3). The basic physics of particle therapy has been reviewed many times [11–18] and is not debated. For many years, however, the cost effectiveness of particle therapy remained controversial because the increased costs compared to X-rays was not matched by level-1 (i.e. derived from randomized phase-III clinical trials) clinical evidence of superiority [19–21].

In recent years, this criticism became weaker. First, cost has been reduced with compact superconducting cyclotrons and single-room treatment facilities [22,23]. Second, evidence showing superiority of charged particles compare to photons in comparative studies is rapidly emerging. Reduced toxicity of protons in head-and-neck tumors has been shown in retrospective analysis in different clinical centers [24–27]. A randomized trial comparing protons to intensity modulated radiotherapy (IMRT) with X-rays for locally advanced esophageal cancer has demonstrated reduced risk and severity of adverse events when

particles are used [28]. Finally, a recent prospective trial has shown increased effectiveness of proton beam therapy in patients treated for leptomeningeal metastasis [29]. Patients with leptomeningeal metastasis, i.e. when cancer spreads to the membranes lining the brain and spinal cord, have a dismal prognosis with a survival of only 3–6 months [30]. Patients treated with protons had improved progression free survival and overall survival compared to those receiving focal X-ray irradiation. This clinical success is entirely due to the physics of protons. With protons, it is possible to have high-dose full craniospinal irradiation that is very toxic with X-rays, because the whole body would be irradiated. Proton craniospinal irradiation is typically employed for treatment of pediatric medulloblastoma (Fig. 4) [31], and can be now a key method to improve survival of patients with leptomeningeal metastasis [32], especially those with reduced genomic variability in circulating tumor DNA [33].

Nevertheless, substantial challenges remain for proton or heavy ion therapy physics. First, even if the cost has been reduced with single-room facilities, it remains substantially higher than photons. Therefore, more compact and cheaper machines remain absolutely necessary to further expand particle therapy [37–39]. Second, even if the sophisticated pencil beam scanning provides excellent coverage of the target, there is a substantial uncertainty on the beam range in the patient [40], entailing large margins around the target that somehow jeopardize the Bragg peak accuracy [41]. The problem is complicated by the organ motion, especially for thoracic tumors, because the movement disrupts the dose distribution. Finally, patient irradiation takes several minutes and is delivered in several daily fractions. Recently, it has been shown in pre-clinical studies that ultra-high dose rates (FLASH radiotherapy) can substantially reduce normal tissue toxicity without affecting tumor control [42]. Beyond the potential biological advantages, ultra-high dose rate can improve the comfort and patient workflow and contribute to solve the organ motion problem. The physical challenge will be to produce particle accelerators and beam delivery systems able to cope with this high-intensity while maintaining conformality.

In short, the current goal is to make particle therapy *cheaper, more conformal* and *faster*. Emerging approaches toward these goals will be summarized here.

## 2 Smaller and cheaper systems

The high investment cost of particle therapy is caused by the complexity of the accelerator, beam transport and delivery technology. The large footprint of these devices brings along high construction costs to satisfy the radiation protection requirements. For this reason, cheaper is almost equivalent to smaller [43]. The most bulky technological components are the accelerator itself (presently either cyclotron plus energy selection system or synchrotron; see Table 1) and the gantry, i.e. the rotating nozzle that allows the delivery of the beam at any angle prescribed in the treatment plan. The size of these machines is determined by the gyroradius  $\rho$  in the Lorentz's formula:

$$B\rho = \frac{p}{q} = \frac{m_0\gamma\beta c}{q} \quad (1)$$

where  $B$  is the magnetic field,  $p$  the momentum and  $q$  the charge of the accelerated particle. In the relativistic expression of the momentum,  $m_0$  is the particle rest mass,  $\beta$  the relative

velocity,  $c$  the speed of light and  $\gamma$  the Lorentz factor. This means that size increases with the particle kinetic energy per nucleon and the mass/charge ratio. Accelerators are designed to reach a desired range in (water-equivalent) tissue, typically 30 cm, which corresponds to a particle-specific kinetic energy, such as 430 MeV/n for carbon or 220 MeV for protons. As shown in Fig. 5, the corresponding magnetic rigidity  $B\rho$  is around 3 times higher for C-ions than for protons. Therapy with ions heavier than protons is therefore associated to larger and more expensive accelerators and gantries.

## 2.1 Current accelerators

The accelerators presently in use in particle therapy are produced by different companies [44,45]. All of these companies are implementing effort to reduce the size of the accelerators. According to Eq. (1), this means increasing  $\mathbf{B}$ , which in turn means using superconducting magnets [46]. Table 2 gives a summary of the main accelerators currently on the market for therapy with protons or carbon ions. Clearly the market focuses on cyclotrons, characterized by a quasi-continuous beam with high intensity and stability; and synchrotrons, whose main advantage is the possibility of actively changing the energy.

Cyclotrons for therapy need to reach high energies, where relativistic effects cannot be neglected. The angular frequency  $\omega$  of the electric field for a particle of charge  $q$  and rest mass  $m_0$  is:

$$\omega = \frac{qB}{\gamma m_0} \quad (2)$$

To cope with the variability of the accelerating frequency in Eq. (2), two strategies are used [47]. In *synchrocyclotrons*, the angular frequency  $\omega$  of the RF is modified to account for the variation of  $\gamma$  with increasing velocity. In *isochronous cyclotrons*,  $\omega$  is kept constant but the magnetic field  $B$  in Eq. (2) is changed. Synchrocyclotrons are smaller and more compact than isochronous cyclotrons, but they have lower output beam current and duty cycle.

Synchrotrons generally use single energy extraction, which requires 1–4 s switching times between energies. Multiple energy extraction, originally developed at NIRS in Japan for C-ions [48], decelerates the beam in discrete steps between short extraction phases so that several energy layers can be delivered in each accelerator spill [49]. This technology reduces the beam deliver time and allows rapid range adaptation without any additional passive energy degrader. Multiple energy extraction reduces beam delivery time also in proton therapy [50] and is indeed implemented in the PROBEAT proton synchrotron (Table 2).

The more stable magnetic field of cyclotrons is more favorable to superconductivity, and it is indeed employed in all modern cyclotrons [45]. While both cyclotrons and synchrotrons are used for protons, until now, only synchrotrons are in use for heavy ions (14 in operation with C-ions by the end of 2022 [9]). However, the C400 IBA compact cyclotron for carbon ions [51] is about to be commissioned in Caen (France) [52].

Proton machines are smaller than those able to accelerate C-ions, and clearly superconducting magnets, usually NbTi, result in more compact accelerators. Yet

superconductivity in a hospital-based center comes with a cost. To achieve high fields ( $B > 3$  T), a large quantity of superconducting material is needed, resulting in high cost and challenging cooling. Magnets in synchrotrons in addition need field ramp rates  $>1$  T/s, a curved shape and usually quadrupole integration [53]. For multiple-energy extraction, fast cycling ( $>10$  Hz) magnets are needed to change energy in small steps, corresponding to the different tumor slices. However, alternating current in superconducting magnets generates eddy currents in the coil and the iron yoke that lead to increased losses and transition to a normal state [54]. High-temperature superconductors can provide a breakthrough in this direction [55], but they are still in experimental testing. Two main candidates are Bi-2212 round wires [56] and rare-earth barium copper oxide (REBCO) coated conductors [57], both theoretically able to reach intensities around 20 T, much higher than those currently achieved with cold superconductors.

## 2.2 Future accelerators

In Table 1 we show other accelerator concepts that may help reducing cost and footprint of future particle therapy facilities.

Radiofrequency linear accelerators were proposed already over 30 years ago by Ugo Amaldi at TERA Foundation and CERN [59,60]. The initial concept was a cyclinac, with a commercial 30 MeV-cyclotron as injector into a 3 GHz linac. However, cyclotrons and linacs have different time structures and the injection is therefore very complex and leads to a large intensity loss (around 95% beam loss in the longitudinal phase space). An all-linac solution can theoretically reach 100% transmission with clean beam dynamics. The TULIP all-linac concept developed at CERN is shown in Fig. 6 [58]. The system is based on the CERN 750 MHz radiofrequency quadrupole (RFQ) that injects 5 MeV particles into an interdigital H-mode cavity. The 10 MeV beam is then accelerated in a 3 GHz drift-tube linac up to 70 MeV followed by a couple-cavity linac up to 230 MeV. The company AVO-ADAM has recently completed a 230 MeV, 16-m long proton linac at the STFC Daresbury laboratory in UK. The accelerator, called LIGHT, is similar to TULIP [61]. Other companies are also working on linac concepts for proton therapy. In principle, linacs can also be used for heavier ions, but their length becomes increasingly long. A project for an advanced compact heavy ion linac with real-time image-guided capability has been recently proposed by the Argonne National Laboratory [62]. An issue of the linacs is the high HF power demand, leading to a low macro cycle of 200 Hz for the current design (Table 1). The AVO-ADAM first hospital-based installation at the Harley Street Proton Therapy Center (Marylebone, London) will show if this leads to problems in clinical application. As the number of involved cavities can be changed from pulse to pulse, in principle very fast energy changes are possible, offering the possibility of online range adaptation and to operate in FLASH regime.

Other concepts described in Table 1, such as the rapid cycling medical synchrotron (RCMS) [63], fixed-field alternating gradient (FFAG) accelerators [64], and the dielectric wall accelerators [65] have been proposed since several years but have not reached the level of industrial production as linacs. The big promise for the future is certainly in laser-driven particle accelerators (LDPA) that have the potential to provide ultra-compact high-intensity

systems for medical applications [66]. The investment in this technology is very high worldwide but, despite many recent efforts for designing beam transport and delivery in therapeutic scenarios [67,68], large problems remain. This includes [69] increasing the intensity and repetition rate; increasing the maximum particle energy; shielding for secondary radiation, especially the very abundant low-energy ions, which is likely to be bulky and expensive; target stability; improving shot-to-shot reproducibility (at least to the few % level); addressing quality-assurance and patient-safety aspects. To date, the highest proton energy ( $\sim 100$  MeV) were achieved at the Vulcan laser of the Rutherford Appleton Laboratory in the UK [70]. Pre-clinical radiobiology studies have been demonstrated at the Draco PW laser in Dresden (Germany), where a mouse ear tumor was treated with  $\sim 60$  MeV protons [71]. Full laser-driven ion medical accelerators remain far in the future, but low-energy linear injectors in ring accelerators could be laser-driven. The current plans for miniaturized synchrotrons in Japan include the use of a short laser-driven particle accelerator as injector for a high-B field superconducting synchrotron [72].

While these new accelerator concept are interesting and have the potential to provide a breakthrough to reduce the footprint of medical accelerators, for the short- and medium-term future it is likely that most of the progress will come from the superconductive magnets.

### 2.3 Beam delivery

Pencil beam scanning is now universally accepted as the beam delivery system for particle therapy (Supplementary video 1). Scanning is essential for intensity-modulated particle therapy (IMPT) and provides a dose conformity which is impossible to obtain with the classical passive scattering method initially used in particle therapy [73]. As we will see in the next section, it brings the problem of interplay between beam and organ motion [74], a problem that still hampers the application of particle therapy to moving organs, especially thoracic tumors. Moreover, 3D volumetric scanning with energy changes is relatively slow and reduces the speed of the treatment.

From the volume/mass point of view, the most massive and expensive element in beam delivery is the rotating gantry. In conventional radiotherapy, the linac itself rotates around the patient. In particle therapy, the gantry is a magnetic system that deflects the beam and can rotate  $360^\circ$  around the patient's couch [47]. Only the Mevion cyclotron (Table 2) is designed to rotate itself around the patient, without additional gantry magnets. A typical proton gantry is about  $10\text{ m} \times 10\text{ m}$  with a weight around 170 tons. As shown in Fig. 5, the size of a C-ion rotating gantry must be much bigger. The first C-ion gantry was installed at the Heidelberg Ion Therapy facility and is a gigantic  $25\text{ m} \times 13\text{ m}$  structure with a weight of 670 tons. The superconductive C-ion gantry at NIRS in Chiba (Japan) is still very big ( $19\text{ m} \times 13\text{ m}$ ) but significantly lighter (300 tons) [83], and the first commercial C-ion Toshiba gantry in operation at Yamagata is still lighter (around 200 tons) [84]. It is possible to further reduce the gantry size using curved canted cosine-tetha superconducting magnets [85], which should be able to reach size comparable to proton gantries [86]. Other projects are studying fixed magnets around the patient, where the beam can be directed on the target from any angle by changing the field strength and beam position [75,87,88] thus eliminating the need of rotating magnets (Fig. 7).

Even with the introduction of superconducting technology, gantries remain one of the most massive and expensive components. Certainly an upright positioning system, where the patient is sitting on a rotating chair, would allow gantryless systems still saving the option of irradiation from multiple angles [89,90]. There is a long history of chairs in particle therapy (Fig. 8), but their use was hampered by imaging, which is normally done in horizontal position. If a patient is planned on a couch, obviously the anatomic changes that occur when moving in vertical position can jeopardize the conformality of the treatment. For these reason, radiation oncologists always included a rotating gantry among the essential requirements for particle therapy, especially for extracranial targets. The Shanghai Proton and Heavy Ion Center is currently irradiating some patients with cranial tumors on a hexapod chair [80]. The use of the chairs is currently expanding thanks to the introduction of vertical CT imaging [91], which is now commercially available (Leo Cancer Care and p-Cure). Irradiation in upright position has the main advantage of being gantryless and therefore substantially cheaper in particle therapy, but an additional advantage is the reduction of organ motion. For lung cancers, MRI [92] and CT [93] studies of healthy volunteers have demonstrated reduced cranio-caudal lung motion and increased lung volume in upright compared to supine position. This suggests that the upright position can lead to a lower mean lung dose. Moreover, a similar reduction in cranio-caudal movement for upper abdomen tumors is expected. Tests of upright position devices in head-and-neck [94] and pelvic [82] cancer patients have demonstrated good reproducibility and improved patient control. A couch will probably remain necessary in clinical practice (e.g. for pediatric patients), but it is likely that irradiation in upright position can reduce the number of gantries needed in a particle therapy center and therefore eventually reduce the costs.

### 3 Highly conformal particle therapy

From the physics point of view, radiotherapy is relatively simple: the goal is to provide the maximum possible dose to the target at the lowest possible dose to the surrounding normal tissue. Dose escalation extends progression-free survival and reduces local recurrence rates, but is limited by normal tissue complications: radiotherapy is not *conformal* enough. The prescribed dose is indeed directed to the planned target volume (PTV), which accounts for the various geometrical uncertainties, such as patient re-positioning and intra- and inter-fraction organ motion. ICRU [95] defines the malignancy visible in the CT as gross-tumor volume (GTV) and its extension to account for microscopic extensions as clinical target volume (CTV). The PTV is an extension of the CTV affected by significant delineation uncertainty [96]. Its contouring is only based on statistical analysis of a small patient population and isotropic extension of the volume of interest [97], not personalized on the individual patient [98]. Ideally, the margin PTV-CTV should be reduced to zero to ensure maximum effectiveness of the treatment.

#### 3.1 Range uncertainty

Thanks to the Bragg peak (Fig. 2), particle therapy is in principle more conformal than X-ray therapy, even in its advanced delivery technologies such as IMRT, tomotherapy or volumetric arc-therapy (VMAT). However, this potential advantage is partly jeopardized by range uncertainty [99]. The prediction of the particle range in the patient is indeed

associated with considerable uncertainties due to imaging, patient setup, beam delivery and dose calculation. Table 3 summarizes some of the sources of range uncertainties and their magnitude for proton therapy [40]. The issues are very similar for heavy ions. Some uncertainties depend on dose calculation, while others do not. A major source of uncertainty is the Bragg peak degradation, caused by tissue inhomogeneities that lead to a wider distal fall-off [100]. This eventually causes an underdosage of the target volume and an overdosage of normal tissue distal to the target volume [101]. A second major contributor is the uncertainty on the mean excitation value  $I$ , which enters directly in the calculation of the beam energy deposition and transport [102,103]. The standard value recommended by ICRU [104] is 75 eV, but values ranging 74.6–81.8 eV are reported in the literature, with an average value  $I = 79.2 \pm 1.6$  eV [105].

Clinically, a substantial margin is added to the distal and proximal target edge in order to ensure tumor coverage, e.g. in proton therapy this range margin is on the order of 3.5% of the prescribed range, based on initial estimation of Michael Goitein at MGH [106]. The additional margin corresponds to a significant normal tissue volume uselessly irradiated with particles that reduces the conformality that would be achieved based on simple physics [41]. If this volume is reduced bringing the PTV close to the CTV, normal tissue complication probability modeling predicts a reduced toxicity for proton [107] and C-ion therapy [108] for both serial and parallel organs at risk.

Using dual-energy X-ray CT for treatment simulation instead of the typically used single-energy X-ray CT can substantially reduce necessary range margins [109], since the two applied photon energy spectra provide partially complementary information on the target tissues. This improves the accuracy of the beam range estimate in the patient [110–112], close to direct particle CT [113].

### 3.2 Moving targets

For IMPT, not delivering homogeneous doses per field, range uncertainties are often not explicitly considered but incorporated into robust optimization strategies designed to minimize the impact of range or setup errors [114]. With robust optimization, the definition of PTV is not necessary any longer and the treatment optimization is done directly on the CTV [115].

Robust optimization is now part of the commercial treatment planning systems in particle therapy. IMPT treatment planning is performed either by single- or multi-field optimization. Single-field is more robust against motion because it only requires the consistency of the anatomy during the treatment delivery of one field, while multi-field optimization requires the integrity of anatomy during the entire treatment session from all treatment fields [116]. Intra-fractional organ motion unavoidably modifies patient anatomy and interferes with the movement of the pencil beam in the scanning pattern. This “interplay effect” degrades the target coverage, generating cold- and hot-spots [74] (Supplementary Video 2). Treatment of moving targets in particle therapy therefore requires motion management techniques aiming to either reduce the anatomical motion (e.g. breath holding or abdominal compression) or to adapt the treatment during planning or delivery (e.g. 4D treatment planning [117], tracking). Despite ongoing attempts to achieve a standardized approach to motion management by



PTCOG [118], currently every center is using its own approach to treat moving targets with IMPT.

Even if breath-holding [119] or compression belts [120] reduce the motion of thoracic and abdominal tumors, these passive methods, routinely used in conventional radiotherapy, have several pitfalls in particle therapy, such as large variability in patient's breath hold capability and compression tolerance. They also do not account for inter-fractional motion [121].

More robust approaches are based on planning on 4DCT images, rather than conventional static CT images [122]. The boundaries of all CTV positions registered in the 4DCT define an internal target volume (ITV). Using the ITV as a static PTV is not adequate in IMPT, considering the interplay effect, the different density of the lung and tumor tissue, range uncertainty and irregular motions and deformations. A valid strategy to mitigate motion-induced range changes is a density override of the ITV [123], which is still in clinical use. ITV can nonetheless be used in association with other motion mitigation strategies, such as rescanning [124], gating [125] or tracking [126]. In beam tracking the motion of the pencil beams accurately follows the motion of the tumor, resulting in the optimal dose distribution comparable to static plan (Supplementary Video 2) [127]. Tracking is, however, technically far more challenging than rescanning or gating. Due to the additional degree of freedom provided by the range of the particles inside the patient, tracking can be performed either only laterally or also in depth, but tracking alone does not regain dose conformity in irregular motion scenarios [128,129]. In addition, as noted above, conformal radiotherapy needs robust optimization and, for proper handling of organ motion, this means 4D robust optimization [130]. These approaches have now been tested both for protons [131,132] and carbon ions [133–135], the latter being further complicated by the problem of non-linearity of the RBE-weighted dose [136] used in heavy ion therapy. The best possible option is the multiphase 4D dose delivery with residual tracking (MP4DRT) [129], where a dedicated quasi-static treatment plan is delivered to each motion phase of a periodic 4DCT and lateral beam tracking compensates for the displacement of the tumor center-of-mass relative to the current phase in the planning 4DCT. MP4DRT can deliver highly conformal particle therapy to irregularly moving targets (Supplementary Video 3), but it depends on clinically available motion monitoring like all tracking-based motion mitigation methods [137].

### 3.3 Online image guidance

Image guidance is generally considered essential for modern, conformal radiotherapy [138]. Modern radiotherapy uses cone beam CT (CBCT) for 3D patient positioning. CBCT reduces re-positioning errors and shows inter-fractional organ movements, but the image quality is lower than for conventional CT, and the image has several artifacts that make a full re-planning difficult. During therapy, optical surface monitoring [139] is offered by different vendors. Orthogonal X-ray fluoroscopy with or without markers and combined with different motion models can be used to track the tumor position. In conventional X-ray therapy, portal imaging of the MV treatment beam is offered on many machines, and is a valuable tool to monitor therapy and to support online dose calculation [140,141]. The combined MR-Linac provides excellent image quality during therapy [142,143], which is also under research for particle therapy [144,145].

All of the above imaging methods identify the target, but do not provide a direct measurement of beam range, which is critical for particle therapy. Current strategies for range estimation rely on different nuclear reactions of the high-energy projectile with the target [146]. The production of positron-emitting isotopes such as  $^{11}\text{C}$  (produced by nuclear fragmentation of the  $^{12}\text{C}$  projectile in carbon ion therapy [147]) or  $^{15}\text{O}$  (generated by target fragmentation of  $^{16}\text{O}$  in proton therapy [148]) with half-lives in the order of minutes enables PET imaging, resulting in 3D images available after delivery [149]. Prompt emission of  $\gamma$ -rays [150] or charged particles [151] provides faster feedback and is currently under clinical investigation [152]. The INSIDE detector at CNAO is currently in use in patients treated with protons or  $^{12}\text{C}$ -ions and includes both an in-beam PET [153] and a dose profiler [154] for the detection of secondary charged particles. However, all these methods are affected by caveats such as low signal-to-noise ratio and indirect correlation to the Bragg Peak that limit their applicability in clinical settings. This justifies the intensive research effort in the field of online range monitoring that is currently ongoing worldwide.

PET imaging is the oldest technique for online beam visualization and range verification, and many new ideas are under study to improve it [156]. These improvements include detection of very short-lived isotopes (such as  $^{12}\text{N}$ ) for online imaging [157], Open-PET with a full-ring geometry developed at NIRS in Japan [158], and J-PET with inexpensive plastic scintillators developed at the Jagellonian University in Poland [159]. A caveat of PET detectors in range verification is the low signal-to-noise ratio because only secondary products are measured, and the shift between the Bragg peak and the activity peak. These problems can be solved using radioactive ion beams for both treatment and beam visualization (Fig. 9). This idea was already proposed many years ago during the pilot trial of heavy ion therapy in Berkeley [160], but was hampered by the low intensity of the radioactive ion beams [161]. With the construction of new, intense accelerators dedicated to nuclear physics with exotic beams [162], a pre-clinical test of this idea becomes possible and is under investigation in the BARB project at GSI in Germany [155,163]. Within BARB, it has been shown that sub-mm resolutions are achievable thanks to the high count rate provided  $^{10}\text{C}$  or  $^{11}\text{C}$  projectiles [164], and a pre-clinical test using an animal model is ongoing.

A novel concept is range probing, which uses selected high energy beams fully penetrating the patient prior to treatment to provide a range verification of setup or control imaging [165,166]. The idea is based on proton radiography [167,168], which is under study since many years to eliminate the problem of the conversion between Hounsfield units (from the CT) to water equivalent path lengths (used in beam transport calculation), but goes toward an online exploitation using simultaneously one beam in the Bragg peak for therapy and second, of lower mass, going through the patient for online imaging. Mixed ion beam guidance has been tested in experiments with subsequent, separate  $^{12}\text{C}$  and  $^4\text{He}$  beams with promising results [169,170].

### 3.4 AI in particle therapy

There is hardly any field of science nowadays where artificial intelligence (AI) methods is not producing rapid advances. Radiotherapy is obviously no exception. Because the

radiotherapy workflow is based on imaging, most AI methods in radiotherapy use deep learning and in particular convolution neural networks. AI can actually be applied in all steps of the radiotherapy chain [171]:

- treatment strategy (machine learning is used in normal tissue complication models [172], radiogenomics [173], and image analysis [174], to support the decisions on individualized treatment strategy);
- segmentation (in the imaging phase, segmentation algorithms reduce the human variability [175]; a notable AI system nnU-Net, a deep learning-based segmentation method that automatically configures itself and adapts to new datasets [176]);
- treatment planning (automatic dose prediction algorithms are already used in conventional radiotherapy [177]);
- QA (machine learning can accelerate treatment plan verification and detect errors for re-planning [178]);
- beam delivery (AI-based algorithms have the potential to monitor organ motion, reduce treatment uncertainty and improve dose delivery accuracy [179]);
- follow-up care (as well as before the treatment, machine learning can support decisions in adjuvant settings [180]).

All these applications in conventional radiotherapy are also venturing into particle therapy. The applications in treatment planning, QA and beam delivery are quite distinct from the problems faced in X-ray therapy, simply because the physics is profoundly different.

Can AI improve *conformality* of particle therapy? First, all methods described for online imaging in Section 3.3 benefit from AI algorithms. For instance, the difference between dose and activity distribution in range verification by PET can be corrected with machine learning algorithms [181,182]. Convolutional neural network can calculate proton dose [183] and improve the resolution of the beam range measurement [184] from prompt- $\gamma$  images; and deep learning can contribute to the development of new methods for range verification such as ionoacoustic [185] or luminescence [186] imaging. Machine learning can also be used to improve CBCT images generating a synthetic CT where it is possible to re-plan the patient [187–189]. Second, machine learning can make dose calculation in treatment planning much faster [190,191], with an accuracy comparable to the time-consuming Monte Carlo calculations. Considering that AI can play a decisive role in online imaging and fast dose calculation, it is clear that it is an ideal tool for online adaptive particle therapy (Fig. 10). Adaptive therapy is a strategy to take into account re-positioning errors, inter-fractional anatomical variations including tumor shrinkage, intra-fractional motions, to make eventually radiotherapy more conformal, as it allows reduction of the margins [192,193]. Adaptive therapy is more necessary in particle therapy than in conventional radiotherapy, because the high precision of the Bragg peak and the steep gradient makes it more sensitive to geometrical uncertainties [194]. It expands to different time scales, because tumor shrinkage can occur over weeks, inter-fractional organ movements and repositioning daily, and intra-fractional movements in the time-scale of seconds. The

clinical workflow, including imaging, segmentation, and treatment planning, makes online adaptation extremely difficult with conventional computational power. Here AI can play a decisive role, both for imaging, generation of synthetic CT and fast dose re-calculation to make particle therapy more conformal. The current results are very promising [195–197] and the rate of progress in this field extremely fast. The need for large training databases to develop new AI methods calls for large, international collaborations between particle therapy facilities, to overcome the limitation that each center treats only a comparatively small number of patients for each cancer site.

## 4 Ultra-high intensities

Soon after the first attempts to use ionizing radiation to sterilize tumors, it became clear that daily dose fractionation was mandatory to reduce the treatment toxicity. The standard fractionation regime requires 2–3 Gy/fraction up to total doses of 60–80 Gy to the target at intensities of 0.5–1 Gy/min. Recently, a paradigm-shift experiment by a French-Swiss collaboration [198] showed that ultra-high dose rates (>40 Gy/s) could spare normal tissue without compromising tumor control. The FLASH effect holds the promise to widen the therapeutic window, and it is therefore currently one of the most prominent topics in radiotherapy. The original experiment was performed with electrons accelerated at a high beam current 4.5 MeV linac. Later the FLASH effect has been observed in different cell and animal models using synchrotron radiation photons [199], hard X-rays [200], protons [201], helium- [202] and carbon- [203] ions. The FLASH effect has a lot of unanswered questions including molecular mechanism, dependence on total dose, instantaneous and average dose rate, irradiation time, fractionation, quantitative assessment of the tissue-dependent dose-modifying factor, let alone the technological challenges [42]. Notwithstanding these uncertainties, clinical trials are ongoing with electrons for cutaneous tumors [204] and protons for bone metastasis [205], and have already shown safety and feasibility of the FLASH approach in the clinical setting.

### 4.1 FLASH impact on medical physics

Whether the FLASH effect will maintain the promise of reducing toxicity and will find wide applications in clinical settings remains to be demonstrated. However, the technological efforts to build machines able to deliver safely high dose at ultra-high dose rate can lead to other benefits from the medical physics side. First, the treatment time is reduced to less than a second, thus potentially improving the clinical workflow, even if the beam-on period is making up only a minor fraction of the time needed to treat the patient (that includes access to the cave, positioning, etc.). Second, FLASH is characterized by high total doses to be delivered in one or 2–4 fractions, and can potentially expand the number of tumor cases for which extreme hypofractionation is feasible today [206]. Again, this results in a benefit for the patient and for the clinics. Finally, FLASH requires a complete re-assessment of the motion management problem [116]. The concept of tumor tracking becomes impossible at the required high delivery speeds, and it also becomes irrelevant. The whole high dose is delivered in a fraction of a second, so the issue is to shoot exactly at the right time when the tumor and the normal organs are in the right position. Fractionation itself is a countermeasure for the interplay effect, because it washes-out the inhomogeneities

over the different fractions, but it is lost in oligofractionated or single-fraction FLASH. Adaptive online therapy and image guidance becomes even more necessary, considering that only intra-fractional but also inter-fractional movements and positioning errors can lead to fatal overdosage in organs at risk. For online imaging, the use of high doses provides an opportunity for pulse-by-pulse imaging using Cherenkov or ionoacoustic imaging [207].

## 4.2 Particle FLASH

Considering the small penetration of electrons from linacs and the poor efficiency of bremsstrahlung for high-intensity X-ray generation, it can be stated that particle therapy is the most mature technology for the clinical translation of FLASH. Clinical cyclotrons can reach FLASH intensities at a fixed energy easily, considering that they have a potential to provide beam currents over an order of magnitude higher than those used in clinical mode (1–10 nA). This is especially true for isochronous cyclotrons with their higher duty cycle, typically achieving beam currents  $\sim 1 \mu\text{A}$ . Synchrotrons used for heavy ion therapy have a low repetition rate ( $\sim 1 \text{ Hz}$ ) and therefore the whole dose has to be delivered in a single synchrotron spill ( $\sim 100 \text{ ms}$ ) [208]. A potential alternative is to use fast extraction, using bunch compression and a kicker magnet to deliver all the particles in the ring in a few  $\mu\text{s}$ , but with this method beam scanning becomes impossible.

For tumor irradiation, the 3D volumetric scanning used in clinics is too slow (each energy change takes  $\sim 1 \text{ s}$ ) to reach FLASH conditions in the whole tumor, and the speed should increase at least two orders of magnitude [209]. The most mature approach for clinical applications of particle is hybrid active–passive systems using patient-specific, 3D-range modulators [210,211]. The pencil beam is scanned in 2D over a ridge filter specifically designed to produce passively the desired SOBP. Irradiation time is therefore only limited by the raster scanning, which is extremely fast. Experimental tests for a lung cancer case demonstrated the delivery of 0.5 Gy to a  $\sim 70 \text{ cm}^3$  target volume in just  $\sim 6 \text{ s}$  at a contemporary heavy ion facility [212]. 3D range modulators are already employed in experimental facilities using protons [213] and heavy ions [214] (Fig. 11) and are currently under test for clinical facilities implementing proton-FLASH [215].

Can particle FLASH be as *conformal* as conventional treatments? Range modulators can replace 3D volumetric scanning with virtually no loss of conformality, but the question is whether a gantry can be used to achieve high conformality with multiple fields. If irradiation is done from multiple angles, the normal tissue surrounding the tissue will experience different dose-rates, ranging from zero (while the gantry is rotated) to the maximum corresponding to the Bragg peak in the distal edge, whereas other sub-volumes will experience intermediate dose-rates due to the overlap of different beamlets [216]. Whether these conditions maintain the FLASH effect is still unclear. One alternative to gantry rotation is to use the toroidal concept described previously in Section 2.3 (Fig. 7), which could be ideal for conformal FLASH. In FLASH treatment planning [217] it will be necessary to include a dose-rate optimization, and perhaps a combination of Bragg peak and shoot-through beams to maintain high dose-rate and conformality [218].

Of course laser-driven particle accelerators, discussed in Section 2.2, would be a prime candidate for FLASH applications. While pre-clinical in vitro cell studies are ongoing [219–

221], the hurdles described in Section 2.2 for clinical translation remain, but it is possible that the investment in FLASH radiotherapy will accelerate the development of appropriate solutions for ultra-high intensity lasers in clinics.

## 5 Conclusions

Particle therapy is growing so quickly (Fig. 1) that we should ask the question of whether it will replace conventional X-ray therapy completely. While the physical and biological (especially for heavy ions) rationale is known since long time, clinical evidence of superiority is now accumulating. Nevertheless, charged particles are not going to replace photons, at least in the near future. The cost of a particle therapy center is in fact still substantially higher than an X-ray linac, and this forces radiation oncologists to select carefully those patient that can benefit the most from particles. Moreover, particle therapy is more sensitive than conventional therapy to positioning uncertainties and organ movements. Finally, with the current outburst of FLASH radiotherapy, particle accelerators should be able reach higher intensity to remain superior to photons and high-energy electron linacs. The future of proton and heavy ion therapy therefore depends on technological improvements to make particle therapy *cheaper, more conformal* and *faster*. Promising solutions include superconductive magnets for more compact accelerators with reduced footprint; irradiation in upright position to avoid large and expensive gantries; AI-assisted online imaging and adaptive radiotherapy to reduce treatment margins; and high-intensity accelerators with 3D-printed range modulators for FLASH radiotherapy. Even if research is ongoing in several centers on these topics, for clinical translation larger collaborative efforts are needed. For example, research in proton radiography is ongoing independently in dozens of proton therapy centers, but as yet they have not produced a single device used in clinical settings. A platform for collaboration in particle therapy is traditionally PTCOG [9], but dedicated funding should come from large-scale initiatives such as the Cancer Moonshot in US [2] or Cancer Mission in EU [3].

## Supplementary Material

Refer to Web version on PubMed Central for supplementary material.

## Acknowledgments

The research in medical physics at GSI is partly funded by EU grant agreements No. 101008548 (HITRIplus), 863969 (RAPTOR) and 883425 (ERC AdG BARB). This paper is dedicated to the memory of Prof. Dr. Gerhard Kraft (1941–2023), founder and former director of the Biophysics Department at GSI and pioneer of heavy ion therapy.

## References

- [1]. Global Burden of Disease Cancer Collaboration. JAMA Oncol. 2019; 5: 1749. doi: 10.1001/jamaoncol.2019.2996 [PubMed: 31560378]
- [2]. Singer DS. Nature Med. 2022; 28: 1345–1347. DOI: 10.1038/s41591-022-01881-5 [PubMed: 35760861]
- [3]. Lawler M, Davies L, Oberst S, Oliver K, Eggermont A, Schmutz A, La Vecchia C, Allemanni C, Lievens Y, Naredi P, Cufer T, et al. Lancet Oncol. 2023; 24: e11–e56. DOI: 10.1016/S1470-2045(22)00540-X [PubMed: 36400101]

- [4]. Thariat J, Hannoun-Levi J-M, Sun Myint A, Vuong T, Gérard J-P. *Nat Rev Clin Oncol*. 2012; 10: 52–60. DOI: 10.1038/nrclinonc.2012.203 [PubMed: 23183635]
- [5]. Chandra RA, Keane FK, Voncken FEM, Thomas CR. *Lancet*. 2021; 398: 171–184. DOI: 10.1016/S0140-6736(21)00233-6 [PubMed: 34166607]
- [6]. Waddle MR, Sio TT, Van Houten HK, Foote RL, Keole SR, Schild SE, Laack N, Daniels TB, Crown W, Shah ND, Miller RC. *Int J Radiat Oncol*. 2017; 99: 1078–1082. DOI: 10.1016/j.ijrobp.2017.07.042
- [7]. Nogueira LM, Jemal A, Yabroff KR, Efstathiou JA. *JAMA Netw Open*. 2022; 5 e229025 doi: 10.1001/jamanetworkopen.2022.9025 [PubMed: 35476066]
- [8]. PTCOG. 2022. accessed December 12, 2022 <http://ptcog.site>
- [9]. PTCOG. 2022. accessed December 12, 2022 <https://www.ptcog.site>
- [10]. Li Y, Li X, Yang J, Wang S, Tang M, Xia J, Gao Y. *Front Oncol*. 2022; 12 doi: 10.3389/fonc.2022.819905
- [11]. Paganetti, H, editor. *Proton Therapy Physics*. second. Taylor Francis; 2019.
- [12]. Schardt D, Elsässer T, Schulz-Ertner D. *Rev Modern Phys*. 2010; 82: 383–425. DOI: 10.1103/RevModPhys.82.383
- [13]. Lomax AJ. *Cancer J*. 2009; 15: 285–291. DOI: 10.1097/PPO.0b013e3181af5cc7 [PubMed: 19672144]
- [14]. Smith AR. *Med Phys*. 2009; 36: 556–568. DOI: 10.1118/1.3058485 [PubMed: 19291995]
- [15]. Durante M, Paganetti H. *Rep Progr Phys*. 2016; 79 096702 doi: 10.1088/0034-4885/79/9/096702
- [16]. Newhauser WD, Zhang R. *Phys Med Biol*. 2015; 60: R155. doi: 10.1088/0031-9155/60/8/R155 [PubMed: 25803097]
- [17]. Kraft G. *Prog Part Nucl Phys*. 2000; 45: 473–544. DOI: 10.1016/S0146-6410(00)00112-5
- [18]. Bichsel H. *Adv Quantum Chem*. 2013; 65: 1–38. DOI: 10.1016/B978-0-12-396455-7.00001-7
- [19]. Lievens Y, Pijls-Johannesma M. *Semin Radiat Oncol*. 2013; 23: 134–141. DOI: 10.1016/j.semradonc.2012.11.005 [PubMed: 23473691]
- [20]. Verma V, Mishra MV, Mehta MP. *Cancer*. 2016; 122: 1483–1501. DOI: 10.1002/cncr.29882 [PubMed: 26828647]
- [21]. Durante M, Orecchia R, Loeffler JS. *Nat Rev Clin Oncol*. 2017; 14: 483–495. DOI: 10.1038/nrclinonc.2017.30 [PubMed: 28290489]
- [22]. Kerstiens J, Johnstone GP, Johnstone PAS. *J Am Coll Radiol*. 2018; 15: 1704–1708. DOI: 10.1016/j.jacr.2018.07.020 [PubMed: 30158085]
- [23]. Contreras J, Zhao T, Perkins S, Sun B, Goddu S, Mutic S, Bottani B, Endicott S, Michalski J, Robinson C, Tsien C, et al. *Pract Radiat Oncol*. 2017; 7: e71–e76. DOI: 10.1016/j.ppro.2016.07.003 [PubMed: 27637138]
- [24]. Li X, Kitpanit S, Lee A, Mah D, Sine K, Sherman EJ, Dunn LA, Michel LS, Fetten J, Zakeri K, Yu Y, et al. *JAMA Netw Open*. 2021; 4 e2113205 doi: 10.1001/jamanetworkopen.2021.13205 [PubMed: 34143193]
- [25]. Youssef I, Yoon J, Mohamed N, Zakeri K, Press RH, Chen L, Gelblum DY, McBride SM, Tsai CJ, Riaz N, Yu Y, et al. *JAMA Netw Open*. 2022; 5 e2241538 doi: 10.1001/jamanetworkopen.2022.41538 [PubMed: 36367724]
- [26]. Baumann BC, Mitra N, Harton JG, Xiao Y, Wojcieszynski AP, Gabriel PE, Zhong H, Geng H, Doucette A, Wei J, O'Dwyer PJ, et al. *JAMA Oncol*. 2020; 6: 237. doi: 10.1001/jamaoncol.2019.4889 [PubMed: 31876914]
- [27]. Baumann BC, Hallahan DE, Michalski JM, Perez CA, Metz JM. *Br Cancer J*. 2020; 123: 869–870. DOI: 10.1038/s41416-0200919-2
- [28]. Lin SH, Hobbs BP, Verma V, Tidwell RS, Smith GL, Lei X, Corsini EM, Mok I, Wei X, Yao L, Wang X, et al. *J Clin Oncol*. 2020; 38: 1569–1579. DOI: 10.1200/JCO.19.02503 [PubMed: 32160096]
- [29]. Yang JT, Wijetunga NA, Pentsova E, Wolden S, Young RJ, Correa D, Zhang Z, Zheng J, Steckler A, Bucwinska W, Bernstein A, et al. *J Clin Oncol*. 2022; 40: 3858–3867. DOI: 10.1200/JCO.22.01148 [PubMed: 35802849]

- [30]. Pan Z, Yang G, He H, Yuan T, Wang Y, Li Y, Shi W, Gao P, Dong L, Zhao G. *Sci Rep*. 2018; 8: 10445. doi: 10.1038/s41598-018-28662-w [PubMed: 29992998]
- [31]. Yock TI, Yeap BY, Ebb DH, Weyman E, Eaton BR, Sherry NA, Jones RM, MacDonald SM, Pulsifer MB, Lavally B, Abrams AN, et al. *Lancet Oncol*. 2016; 17: 287–298. DOI: 10.1016/S1470-2045(15)00167-9 [PubMed: 26830377]
- [32]. Barden MM, Omuro AM. *Cancer*. 2023; doi: 10.1002/cncr.34711
- [33]. Wijetunga NA, Goglia AG, Weinhold N, Berger MF, Cislo M, Higginson DS, Chabot K, Osman AM, Schaff L, Pentsova E, Miller AM, et al. *Clin Cancer Res*. 2022; OF1–OF9. DOI: 10.1158/1078-0432.CCR-22-2434
- [34]. Faddegon B, Ramos-Méndez J, Schuemann J, McNamara A, Shin J, Perl J, Paganetti H. *Phys Medica*. 2020; 72: 114–121. DOI: 10.1016/j.ejmp.2020.03.019
- [35]. Krämer M, Jäkel O, Haberer T, Kraft G, Schardt D, Weber U. *Phys Med Biol*. 2000; 45: 3299–3317. DOI: 10.1088/0031-9155/45/11/313 [PubMed: 11098905]
- [36]. Wieser H-P, Cisternas E, Wahl N, Ulrich S, Stadler A, Mescher H, Müller L-R, Klinge T, Gabrys H, Burigo L, Mairani A, et al. *Med Phys*. 2017; 44: 2556–2568. DOI: 10.1002/mp.12251 [PubMed: 28370020]
- [37]. Bortfeld TR, Loeffler JS. *Nature*. 2017; 549: 451–453. DOI: 10.1038/549451a [PubMed: 28959981]
- [38]. Shah A, Ricci KI, Efstathiou JA. *Lancet Oncol*. 2016; 17: 559–561. DOI: 10.1016/S1470-2045(16)00171-6 [PubMed: 27301029]
- [39]. Mitin T, Zietman AL. *J Clin Oncol*. 2014; 32: 2855–2863. DOI: 10.1200/JCO.2014.55.1945 [PubMed: 25113772]
- [40]. Paganetti H. *Phys Med Biol*. 2012; 57: R99–R117. DOI: 10.1088/0031-9155/57/11/R99 [PubMed: 22571913]
- [41]. Durante M, Flanz J. *Semin Oncol*. 2019; 46: 219–225. DOI: 10.1053/j.seminoncol.2019.07.007 [PubMed: 31451308]
- [42]. Vozenin M-C, Bourhis J, Durante M. *Nat Rev Clin Oncol*. 2022; 19: 791–803. DOI: 10.1038/s41571-022-00697-z [PubMed: 36303024]
- [43]. Durante M, Debus J, Loeffler JS. *Nat Rev Phys*. 2021; 3: 777–790. DOI: 10.1038/s42254-021-00368-5 [PubMed: 34870097]
- [44]. Coutrakon GB. *Technol Cancer Res Treat*. 2007; 6: 49–54. DOI: 10.1177/15330346070060S408
- [45]. Collings EW, Lu L, Gupta N, Sumption MD. *Front Oncol*. 2022; 11 doi: 10.3389/fonc.2021.737837
- [46]. Alonso JR, Antaya TA. *Rev Accel Sci Technol, WORLD SCIENTIFIC*. 2013; 227–263. DOI: 10.1142/9789814449953\_0009
- [47]. Owen H, Holder D, Alonso J, Mackay R. *Internat J Modern Phys A*. 2013; 29: 1–54. DOI: 10.1142/S0217751X14410024
- [48]. Iwata Y, Kadowaki T, Uchiyama H, Fujimoto T, Takada E, Shirai T, Furukawa T, Mizushima K, Takeshita E, Katagiri K, Sato S, et al. *Nucl Instrum Methods Phys Res A*. 2010; 624: 33–38. DOI: 10.1016/j.nima.2010.09.016
- [49]. Mizushima K, Furukawa T, Iwata Y, Hara Y, Saotome N, Saraya Y, Tansho R, Sato S, Fujimoto T, Shirai T, Noda K. *Nucl Instrum Methods Phys Res B*. 2017; 406: 347–351. DOI: 10.1016/j.nimb.2017.03.051
- [50]. Younkin JE, Bues M, Sio TT, Liu W, Ding X, Keole SR, Stoker JB, Shen J. *Adv Radiat Oncol*. 2018; 3: 412–420. DOI: 10.1016/j.adro.2018.02.006 [PubMed: 30197942]
- [51]. Jongen Y, Abs M, Blondin A, Kleeven W, Zaremba S, Vandeplasseche D, Aleksandrov V, Gursky S, Karamyshev O, Karamysheva G, Kazarinov N, et al. *Nucl Instrum Methods Phys Res A*. 2010; 624: 47–53. DOI: 10.1016/j.nima.2010.09.028
- [52]. Chevalier F, Lesueur P, Gaubert G. *Nucl Phys News*. 2022; 32: 27–31. DOI: 10.1080/10619127.2022.2063002
- [53]. Rossi L, Ballarino A, Barna D, Benedetto E, Calzolaio C, Ceruti G, De Matteis E, Echeandia A, Ekelof T, Farinon S, Felcini E, et al. *IEEE Trans Appl Supercond*. 2022; 32: 1–7. DOI: 10.1109/TASC.2022.3147433



- [54]. Ageev A, Bogdanov I, Kozub S, Tkachenko L. Nucl Instrum Methods Phys Res A. 2021; 1000 165223 doi: 10.1016/j.nima.2021.165223
- [55]. Baird YTE, Li Q. IEEE Trans Appl Supercond. 2020; 30: 1–8. DOI: 10.1109/TASC.2019.2954681
- [56]. Larbalestier DC, Jiang J, Trociewitz UP, Kametani F, Scheuerlein C, Dalban-Canassy M, Matras M, Chen P, Craig NC, Lee PJ, Hellstrom EE. Nature Mater. 2014; 13: 375–381. DOI: 10.1038/nmat3887 [PubMed: 24608141]
- [57]. Wang X, Gourlay SA, Prestemon SO. Instruments. 2019; 3: 62. doi: 10.3390/instruments3040062
- [58]. Benedetti S, Grudiev A, Latina A. Phys Rev Accel Beams. 2017; 20 040101 doi: 10.1103/PhysRevAccelBeams.20.040101
- [59]. Amaldi U, Braccini S, Puggioni P. Rev Accel Sci Technol. 2009; 2: 111–131. DOI: 10.1142/S179362680900020X
- [60]. Amaldi U, Bonomi R, Braccini S, Crescenti M, Degiovanni A, Garlasch M, Garonna A, Magrin G, Mellace C, Pearce P, Pittá G, et al. Nucl Instrum Methods Phys Res A. 2010; 620: 563–577. DOI: 10.1016/j.nima.2010.03.130
- [61]. Degiovanni, A. 9th Int. Part. Accel. Conf; Vancouver, Canada. 2018. 425–428.
- [62]. Mustapha B, Aydogan B, Nolen J, Nassiri A, Noonan J, Pankuch M, Welsh J, Schulte R, Robb J. AIP Conf Proc. 2019; 050009 doi: 10.1063/1.5127701
- [63]. Trbojevic, D, Alessi, J, Blaskiewicz, M, Cullen, C, Hahn, H, Lowenstein, D, Marneris, I, Meng, W, Mi, J, Pai, C, Raparia, D. , et al. Proc IPAC. San Sebastian; Spain: 2011.
- [64]. Antoine S, Autin B, Beeckman W, Collot J, Conjat M, Forest F, Fourrier J, Froidefond E, Lancelot JL, Mandrillon J, Mandrillon P, et al. Nucl Instrum Methods Phys Res A. 2009; 602: 293–305. DOI: 10.1016/j.nima.2009.01.025
- [65]. Caporaso GJ, Chen Y-J, Sampayan SE. Rev Accel Sci Technol. 2009; 02: 253–263. DOI: 10.1142/S1793626809000235
- [66]. Badziak J. J Phys Conf Ser. 2018; 959 012001 doi: 10.1088/1742-6596/959/1/012001
- [67]. Wang KD, Zhu K, Easton MJ, Li YJ, Lin C, Yan XQ. Phys Rev Accel Beams. 2020; 23 111302 doi: 10.1103/PhysRevAccelBeams.23.111302
- [68]. Karsch L, Beyreuther E, Enghardt W, Gotz M, Masood U, Schramm U, Zeil K, Pawelke J. Acta Oncol (Madr). 2017; 56: 1359–1366. DOI: 10.1080/0284186X.2017.1355111
- [69]. Linz U, Alonso J. Phys Rev Accel Beams. 2016; 19 124802 doi: 10.1103/PhysRevAccelBeams.19.124802
- [70]. Higginson A, Gray RJ, King M, Dance RJ, Williamson SDR, Butler NMH, Wilson R, Capdessus R, Armstrong C, Green JS, Hawkes SJ, et al. Nature Commun. 2018; 9: 724. doi: 10.1038/s41467-018-03063-9 [PubMed: 29463872]
- [71]. Kroll F, Brack F-E, Bernert C, Bock S, Bodenstern E, Brüchner K, Cowan TE, Gaus L, Gebhardt R, Helbig U, Karsch L, et al. Nat Phys. 2022; 18: 316–322. DOI: 10.1038/s41567-022-01520-3
- [72]. Noda K. J Phys Conf Ser. 2019; 1154 012019 doi: 10.1088/1742-6596/1154/1/012019
- [73]. Lomax AJ, Boehringer T, Coray A, Egger E, Goitein G, Grossmann M, Juelke P, Lin S, Pedroni E, Rohrer B, Roser W, et al. Med Phys. 2001; 28: 317–324. DOI: 10.1118/1.1350587 [PubMed: 11318312]
- [74]. Bert C, Durante M. Phys Med Biol. 2011; 56: R113–R144. DOI: 10.1088/0031-9155/56/16/R01 [PubMed: 21775795]
- [75]. Bottura L, Felcini E, Ferrero V, Fiorina E, Monaco V, Pennazio F, de Rijk G, Cerello P. Front Phys. 2020; 8 doi: 10.3389/fphy.2020.566679
- [76]. Kamada T, Tsujii H, Mizoe J-E, Matsuoka Y, Tsuji H, Osaka Y, Minohara S, Miyahara N, Endo M, Kanai T. Radiother Oncol. 1999; 50: 235–237. DOI: 10.1016/S0167-8140(99)00005-5 [PubMed: 10368048]
- [77]. Heeg, P; Schardt, D; Störmer, J. GSI Rep 2002-1, GSI, Darmstadt. 2002. 166
- [78]. Schreuder, N. Technological Developments Allowing for the Widespread Clinical Adoption of Proton Radiotherapy. University College London; 2020. [https://discovery.ucl.ac.uk/id/eprint/10118672/1/Schreuder\\_NiekschreuderPHDThesis-GrandFinalJan52021.pdf](https://discovery.ucl.ac.uk/id/eprint/10118672/1/Schreuder_NiekschreuderPHDThesis-GrandFinalJan52021.pdf)

- [79]. Balakin VE, Belikhin MA, Pryanichnikov AA, Shemyakov AE, Strelnikova NS. *KnE Energy*. 2018; 3: 45. doi: 10.18502/ken.v3i2.1790
- [80]. Sheng Y, Sun J, Wang W, Stuart B, Kong L, Gao J, You D, Wu X. *Front Oncol*. 2020; 10 doi: 10.3389/fonc.2020.00122
- [81]. Buchner T, Yan S, Li S, Flanz J, Hueso-Gonzalez F, Kielty E, Bortfeld T, Rus D. *Biomechatronics*; 2020 8th IEEE RAS/EMBS Int. Conf. Biomed. Robot; 2020. 981–988.
- [82]. Boisbouvier S, Boucaud A, Tanguy R, Grégoire V. *Tech Innov Patient Support Radiat Oncol*. 2022; 24: 124–130. DOI: 10.1016/j.tipsro.2022.11.003 [PubMed: 36471684]
- [83]. Noda K, Furukawa T, Fujimoto T, Hara Y, Inaniwa T, Iwata Y, Katagiri K, Kanematsu N, Mizushima K, Mori S, Saotome N, et al. *Nucl Instrum Methods Phys Res B*. 2017; 406: 374–378. DOI: 10.1016/j.nimb.2017.04.021
- [84]. Zhou Y, Li Y, Kubota Y, Sakai M, Ohno T. *Front Oncol*. 2021; 11 doi: 10.3389/fonc.2021.715025
- [85]. Wan W, Brouwer L, Caspi S, Prestemon S, Gerbershagen A, Schippers JM, Robin D. *Phys Rev Spec Top-Accel Beams*. 2015; 18 103501 doi: 10.1103/PhysRevSTAB.18.103501
- [86]. Kim J, Yoon M. *Phys Rev Accel Beams*. 2019; 22 101601 doi: 10.1103/PhysRevAccelBeams.22.101601
- [87]. Nesteruk KP, Bolsi A, Lomax AJ, Meer D, van de Water S, Schippers JM. *Phys Med Biol*. 2021; 66 055018 doi: 10.1088/1361-6560/abe02b [PubMed: 33498040]
- [88]. Felcini E, Haziot A, Louzguiti A, Lehtinen T, Vernassa G, Dutoit B, Bottura L. *IEEE Trans Appl Supercond*. 2022; 32: 1–5. DOI: 10.1109/TASC.2022.3160380
- [89]. Volz L, Sheng Y, Durante M, Graeff C. *Front Oncol*. 2022; 12 doi: 10.3389/fonc.2022.930850
- [90]. Rahim S, Korte J, Hardcastle N, Hegarty S, Kron T, Everitt S. *Front Oncol*. 2020; 10 doi: 10.3389/fonc.2020.00213
- [91]. Shah AP, Strauss JB, Kirk MC, Chen SS, Kroc TK, Zusag TW. *Med Dosim*. 2009; 34: 82–86. DOI: 10.1016/j.meddos.2008.05.004 [PubMed: 19181260]
- [92]. Yang J, Chu D, Dong L, Court LE. *Pract Radiat Oncol*. 2014; 4: e53–e58. DOI: 10.1016/j.prro.2013.04.005 [PubMed: 24621432]
- [93]. Yamada Y, Yamada M, Chubachi S, Yokoyama Y, Matsuoka S, Tanabe A, Nijijima Y, Murata M, Fukunaga K, Jinzaki M. *Sci Rep*. 2020; 10 16203 doi: 10.1038/s41598-020-73240-8 [PubMed: 33004894]
- [94]. McCarroll RE, Beadle BM, Fullen D, Balter PA, Followill DS, Stingo FC, Yang J, Court LE. *J Appl Clin Med Phys*. 2017; 18: 223–229. DOI: 10.1002/acm2.12024 [PubMed: 28291911]
- [95]. ICRU. *J ICRU*. 2010; 10 doi: 10.1093/jicru/10.1.Report83
- [96]. Segedin B, Petric P. *Radiol Oncol*. 2016; 50: 254–262. DOI: 10.1515/raon-2016-0023 [PubMed: 27679540]
- [97]. van Herk M, Remeijer P, Rasch C, Lebesque JV. *Int J Radiat Oncol*. 2000; 47: 1121–1135. DOI: 10.1016/S0360-3016(00)00518-6
- [98]. Bernstein D, Taylor A, Nill S, Oelfke U. *Phys Med Biol*. 2021; 66 055024 doi: 10.1088/1361-6560/abe029 [PubMed: 33498018]
- [99]. Lomax AJ. *Br J Radiol*. 2020; 93 20190582 doi: 10.1259/bjr.20190582 [PubMed: 31778317]
- [100]. Urie M, Goitein M, Holley WR, Chen GTY. *Phys Med Biol*. 1986; 31: 1–15. DOI: 10.1088/0031-9155/31/1/001 [PubMed: 3952143]
- [101]. Sawakuchi GO, Titt U, Mirkovic D, Mohan R. *Phys Med Biol*. 2008; 53: 4605–4619. DOI: 10.1088/0031-9155/53/17/010 [PubMed: 18678928]
- [102]. Besemer A, Paganetti H, Bednarz B. *Phys Med Biol*. 2013; 58: 887–902. DOI: 10.1088/0031-9155/58/4/887 [PubMed: 23337713]
- [103]. Kamakura S, Sakamoto N, Ogawa H, Tsuchida H, Inokuti M. *J Appl Phys*. 2006; 100 064905 doi: 10.1063/1.2345478
- [104]. Deasy J. *Med Phys*. 1994; 21: 709–710. DOI: 10.1118/1.597176
- [105]. Paul H. *Adv Quantum Chem*. 2013; 65: 39–61. DOI: 10.1016/B978-0-12-396455-7.00002-9
- [106]. Goitein M. *Med Phys*. 1985; 12: 608–612. DOI: 10.1118/1.595762 [PubMed: 4046996]

- [107]. Tattenberg S, Madden TM, Gorissen BL, Bortfeld T, Parodi K, Verburg J. *Med Phys*. 2021; mp.15097 doi: 10.1002/mp.15097
- [108]. Sokol O, Cella L, Boscolo D, Horst F, Oliviero C, Pacelli R, Palma G, De Simoni M, Conson M, Caroprese M, Weber U, et al. *Sci Rep*. 2022; 12 21792 doi: 10.1038/s41598-022-26290-z [PubMed: 36526710]
- [109]. Peters N, Wohlfahrt P, Hofmann C, Möhler C, Menkel S, Tschiche M, Krause M, Troost EGC, Enghardt W, Richter C. *Radiother Oncol*. 2022; 166: 71–78. DOI: 10.1016/j.radonc.2021.11.002 [PubMed: 34774653]
- [110]. Bär E, Lalonde A, Royle G, Lu H-M, Bouchard H. *Med Phys*. 2017; 44: 2332–2344. DOI: 10.1002/mp.12215 [PubMed: 28295434]
- [111]. Niepel KB, Stanislawski M, Wuerl M, Doerringer F, Pinto M, Dietrich O, Ertl-Wagner B, Lalonde A, Bouchard H, Pappas E, Yohannes I, et al. *Phys Med Biol*. 2021; 66 075009 doi: 10.1088/1361-6560/abd14
- [112]. Berthold J, Khamfongkhrua C, Petzoldt J, Thiele J, Hölscher T, Wohlfahrt P, Peters N, Jost A, Hofmann C, Janssens G, Smeets J, et al. *Int J Radiat Oncol*. 2021; 111: 1033–1043. DOI: 10.1016/j.ijrobp.2021.06.036
- [113]. Volz L, Collins-Fekete C-A, Bär E, Brons S, Graeff C, Johnson RP, Runz A, Sarosiek C, Schulte RW, Seco J. *Phys Med Biol*. 2021; 66 235010 doi: 10.1088/1361-6560/ac33ec
- [114]. Unkelbach J, Paganetti H. *Semin Radiat Oncol*. 2018; 28: 88–96. DOI: 10.1016/j.semradonc.2017.11.005 [PubMed: 29735195]
- [115]. Unkelbach J, Alber M, Bangert M, Bokrantz R, Chan TCY, Deasy JO, Fredriksson A, Gorissen BL, van Herk M, Liu W, Mahmoudzadeh H, Nohadani O, et al. *Phys Med Biol*. 2018; 63 22TR02 doi: 10.1088/1361-6560/aae659
- [116]. Pakela JM, Knopf A, Dong L, Rucinski A, Zou W. *Front Oncol*. 2022; 12 doi: 10.3389/fonc.2022.806153
- [117]. Richter D, Schwarzkopf A, Trautmann J, Krämer M, Durante M, Jäkel O, Bert C. *Med Phys*. 2013; 40 051722 doi: 10.1118/1.4800802 [PubMed: 23635270]
- [118]. Chang JY, Zhang X, Knopf A, Li H, Mori S, Dong L, Lu H-M, Liu W, Badiyan SN, Both S, Meijers A, et al. *Int J Radiat Oncol*. 2017; 99: 41–50. DOI: 10.1016/j.ijrobp.2017.05.014
- [119]. Dueck J, Knopf A-C, Lomax A, Albertini F, Persson GF, Josipovic M, Aznar M, Weber DC, Munckaf Rosenschöld P. *Int J Radiat Oncol*. 2016; 95: 534–541. DOI: 10.1016/j.ijrobp.2015.11.015
- [120]. Lin L, Souris K, Kang M, Glick A, Lin H, Huang S, Stützer K, Janssens G, Sterpin E, Lee JA, Solberg TD, et al. *Med Phys*. 2017; 44: 703–712. DOI: 10.1002/mp.12040 [PubMed: 28133755]
- [121]. Mori S, Lu H-M, Wolfgang JA, Choi NC, Chen GTY. *J Radiat Res*. 2009; 50: 513–519. DOI: 10.1269/jrr.09032 [PubMed: 19959880]
- [122]. Czerska K, Emert F, Kopec R, Langen K, McClelland JR, Meijers A, Miyamoto N, Riboldi M, Shimizu S, Terunuma T, Zou W, et al. *Phys Medica*. 2021; 82: 54–63. DOI: 10.1016/j.ejmp.2020.12.013
- [123]. Kang Y, Zhang X, Chang JY, Wang H, Wei X, Liao Z, Komaki R, Cox JD, Balter PA, Liu H, Zhu XR, et al. *Int J Radiat Oncol*. 2007; 67: 906–914. DOI: 10.1016/j.ijrobp.2006.10.045
- [124]. Grassberger C, Dowdell S, Sharp G, Paganetti H. *Med Phys*. 2015; 42: 2462–2469. DOI: 10.1118/1.4916662 [PubMed: 25979039]
- [125]. Steidl P, Haberer T, Durante M, Bert C. *Phys Med Biol*. 2013; 58: N295–N302. DOI: 10.1088/0031-9155/58/21/N295 [PubMed: 24141025]
- [126]. Prunaretty J, Boisselier P, Aillères N, Riou O, Simeon S, Bedos L, Azria D, Fenoglietto P. *Rep Pract Oncol Radiother*. 2019; 24: 97–104. DOI: 10.1016/j.rpor.2018.11.003 [PubMed: 30532657]
- [127]. Luchtenborg R, Saito N, Durante M, Bert C. *Med Phys*. 2011; 38: 5448–5458. DOI: 10.1118/1.3633891 [PubMed: 21992364]
- [128]. Krieger M, Giger A, Jud C, Duetschler A, Salomir R, Bieri O, Bauman G, Nguyen D, Cattin PC, Weber DC, Lomax AJ, et al. *Phys Med Biol*. 2021; 66 035011 doi: 10.1088/1361-6560/abcde6 [PubMed: 33238246]

- [129]. Steinsberger T, Donetti M, Lis M, Volz L, Wolf M, Durante M, Graeff C. *Int J Radiat Oncol.* 2022; doi: 10.1016/j.ijrobp.2022.11.034
- [130]. Graeff C. *Phys Medica.* 2014; 30: 570–577. DOI: 10.1016/j.ejmp.2014.03.011
- [131]. Ge S, Wang X, Liao Z, Zhang L, Sahoo N, Yang J, Guan F, Mohan R. *Cancers (Basel).* 2019; 11: 35. doi: 10.3390/cancers11010035 [PubMed: 30609652]
- [132]. Liu W, Schild SE, Chang JY, Liao Z, Chang Y-H, Wen Z, Shen J, Stoker JB, Ding X, Hu Y, Sahoo N, et al. *Int J Radiat Oncol.* 2016; 95: 523–533. DOI: 10.1016/j.ijrobp.2015.11.002
- [133]. Graeff C, Lüchtenborg R, Eley JG, Durante M, Bert C. *Radiother Oncol.* 2013; 109: 419–424. DOI: 10.1016/j.radonc.2013.09.018 [PubMed: 24183865]
- [134]. Lis M, Donetti M, Newhauser W, Durante M, Dey J, Weber U, Wolf M, Steinsberger T, Graeff C. *Phys Medica.* 2020; 76: 307–316. DOI: 10.1016/j.ejmp.2020.07.029
- [135]. Knopf A-C, Czerska K, Fracchiolla F, Graeff C, Molinelli S, Rinaldi I, Rucincki A, Sterpin E, Stützer K, Trnkova P, Zhang Y, Chang JY, et al. *Radiother Oncol.* 2022; 169: 77–85. DOI: 10.1016/j.radonc.2022.02.018 [PubMed: 35189152]
- [136]. Molinelli S, Magro G, Mairani A, Matsufuji N, Kanematsu N, Inaniwa T, Mirandola A, Russo S, Mastella E, Hasegawa A, Tsuji H, et al. *Radiother Oncol.* 2016; 120: 307–312. DOI: 10.1016/j.radonc.2016.05.031 [PubMed: 27394694]
- [137]. Riboldi M, Orecchia PR, Baroni PG. *Lancet Oncol.* 2012; 13: e383–e391. DOI: 10.1016/S1470-2045(12)70243-7 [PubMed: 22935238]
- [138]. Grégoire V, Guckenberger M, Haustermans K, Lagendijk JJW, Ménard C, Pötter R, Slotman BJ, Tanderup K, Thorwarth D, Herk M, Zips D. *Mol Oncol.* 2020; 14: 1470–1491. DOI: 10.1002/1878-0261.12751 [PubMed: 32536001]
- [139]. Fattori G, Hrbacek J, Regele H, Bula C, Mayor A, Danuser S, Oxley DC, Rechsteiner U, Grossmann M, Via R, Böhlen TT, et al. *Z Med Phys.* 2022; 32: 52–62. DOI: 10.1016/j.zemedi.2020.07.001 [PubMed: 32830006]
- [140]. Mijnheer B, Beddar S, Izewska J, Reft C. *Med Phys.* 2013; 40: 070903 doi: 10.1118/1.4811216 [PubMed: 23822404]
- [141]. Olaciregui-Ruiz I, Beddar S, Greer P, Jornet N, McCurdy B, Paiva-Fonseca G, Mijnheer B, Verhaegen F. *Phys Imaging Radiat Oncol.* 2020; 15: 108–116. DOI: 10.1016/j.phro.2020.08.003 [PubMed: 33458335]
- [142]. Raaymakers BW, Jürgenliemk-Schulz IM, Bol GH, Glitzner MA, Kotte NTJ, van Asselen B, de Boer JCJ, Bluemink JJ, Hackett SL, Moerland MA, Woodings SJ, et al. *Phys Med Biol.* 2017; 62: L41–L50 doi: 10.1088/1361-6560/aa9517 [PubMed: 29135471]
- [143]. Bayouth JE, Low DA, Zaidi H. *Med Phys.* 2019; 46: 3753–3756. DOI: 10.1002/mp.13657 [PubMed: 31199516]
- [144]. Pham TT, Whelan B, Oborn BM, Delaney GP, Vinod S, Brighi C, Barton M, Keall P. *Radiother Oncol.* 2022; 170: 37–47. DOI: 10.1016/j.radonc.2022.02.031 [PubMed: 35257848]
- [145]. Moteabbed M, Smeets J, Hong TS, Janssens G, Labarbe R, Wolfgang JA, Bortfeld TR. *Phys Med Biol.* 2021; 66: 195004 doi: 10.1088/1361-6560/ac1ef2
- [146]. Kraan AC. *Front Oncol.* 2015; 5: 150. doi: 10.3389/fonc.2015.00150 [PubMed: 26217586]
- [147]. Pönisch F, Parodi K, Hasch BG, Enghardt W. *Phys Med Biol.* 2004; 49: 5217–5232. accessed June 13, 2017 [PubMed: 15656273]
- [148]. Zhu X, El Fakhri G. *Theranostics.* 2013; 3: 731–740. DOI: 10.7150/thno.5162 [PubMed: 24312147]
- [149]. Parodi K. *Med Phys.* 2015; 42: 7153–7168. DOI: 10.1118/1.4935869 [PubMed: 26632070]
- [150]. Krimmer J, Dauvergne D, Létang JM, Testa É. *Nucl Instrum Methods Phys Res A.* 2018; 878: 58–73. DOI: 10.1016/j.nima.2017.07.063
- [151]. Piersanti L, Bellini F, Bini F, Collamati F, De Lucia E, Durante M, Faccini R, Ferroni F, Fiore S, Iarocci E, La Tessa C, et al. *Phys Med Biol.* 2014; 59: 1857–1872. [PubMed: 24625560]
- [152]. Hueso-González F, Enghardt W, Fiedler F, Golnik C, Janssens G, Petzoldt J, Prieels D, Priegnitz M, Römer KE, Smeets J, Vander Stappen F, et al. *Phys Med Biol.* 2015; 60: 6247–6272. DOI: 10.1088/0031-9155/60/16/6247 [PubMed: 26237433]

- [153]. Moglioni M, Kraan AC, Baroni G, Battistoni G, Belcari N, Berti A, Carra P, Cerello P, Ciocca M, De Gregorio A, De Simoni M, et al. *Front Oncol.* 2022; 12 doi: 10.3389/fonc.2022.929949
- [154]. Toppi M, Baroni G, Battistoni G, Bisogni MG, Cerello P, Ciocca M, De Maria P, De Simoni M, Donetti M, Dong Y, Embriaco A, et al. *Front Oncol.* 2021; 11 doi: 10.3389/fonc.2021.601784
- [155]. Boscolo D, Kostyleva D, Safari MJ, Anagnostatou V, Äystö J, Bagchi S, Binder T, Dedes G, Dendooven P, Dickel T, Drozd V, et al. *Front Oncol.* 2021; 11 doi: 10.3389/fonc.2021.737050
- [156]. Parodi K, Yamaya T, Moskal P. *Z Med Phys.* 2022; doi: 10.1016/j.zemedi.2022.11.001
- [157]. Buitenhuis HJT, Diblen F, Brzezinski KW, Brandenburg S, Dendooven P. *Phys Med Biol.* 2017; 62: 4654–4672. DOI: 10.1088/1361-6560/aa6b8c [PubMed: 28379155]
- [158]. Tashima H, Yoshida E, Inadama N, Nishikido F, Nakajima Y, Wakizaka H, Shinaji T, Nitta M, Kinouchi S, Suga M, Haneishi H, et al. *Phys Med Biol.* 2016; 61: 1795–1809. DOI: 10.1088/0031-9155/61/4/1795 [PubMed: 26854528]
- [159]. Borys D, Baran J, Brzeziński K, Gajewski J, Chug N, Coussat A, Czerwiński E, Dadgar M, Dulski K, Eliyan KV, Gajos A, et al. *Phys Med Biol.* 2022; 67 224002 doi: 10.1088/1361-6560/ac944c
- [160]. Llacer J, Chatterjee A, Alpen EL, Saunders W, Andreae S, Jackson HC. *IEEE Trans Med Imaging.* 1984; 3: 80–90. DOI: 10.1109/TMI.1984.4307660 [PubMed: 18234615]
- [161]. Durante M, Parodi K. *Front Phys.* 2020; 8 00326 doi: 10.3389/fphy.2020.00326 [PubMed: 33224941]
- [162]. Durante M, Golubev A, Park W-Y, Trautmann C. *Phys Rep.* 2019; 800: 1–37. DOI: 10.1016/j.physrep.2019.01.004
- [163]. Boscolo D, Kostyleva D, Schuy C, Weber U, Haettner E, Purushothaman S, Dendooven P, Dickel T, Drozd V, Franczack B, Geissel H, et al. *Nucl Instrum Methods Phys Res A.* 2022; 1043 167464 doi: 10.1016/j.nima.2022.167464 [PubMed: 36345417]
- [164]. Kostyleva D, Purushothaman S, Dendooven P, Haettner E, Geissel H, Ozoemelum I, Schuy C, Weber U, Boscolo D, Dickel T, Drozd V, et al. *Phys Med Biol.* 2023; 68 015003 doi: 10.1088/1361-6560/aca5e8
- [165]. Farace P, Righetto R, Meijers A. *Phys Med Biol.* 2016; 61: 4078–4087. DOI: 10.1088/0031-9155/61/11/4078 [PubMed: 27164479]
- [166]. Seller Oria C, Thummerer A, Free J, Langendijk JA, Both S, Knopf AC, Meijers A. *Med Phys.* 2021; 48: 4498–4505. DOI: 10.1002/mp.15020 [PubMed: 34077554]
- [167]. Poludniowski G, Allinson NM, Evans PM. *Br J Radiol.* 2015; 88 20150134 doi: 10.1259/bjr.20150134 [PubMed: 26043157]
- [168]. Johnson RP. *Rep Progr Phys.* 2018; 81 016701 doi: 10.1088/1361-6633/aa8b1d
- [169]. Mazzucconi D, Agosteo S, Ferrarini M, Fontana L, Lante V, Pullia M, Savazzi S. *Med Phys.* 2018; 45: 5234–5243. DOI: 10.1002/mp.13219 [PubMed: 30269349]
- [170]. Volz L, Kelleter L, Brons S, Burigo L, Graeff C, Niebuhr NI, Radogna R, Scheloske S, Schömers C, Jolly S, Seco J. *Phys Med Biol.* 2020; 65 055002 doi: 10.1088/1361-6560/ab6e52 [PubMed: 31962302]
- [171]. Huynh E, Hosny A, Guthier C, Bitterman DS, Petit SF, Haas-Kogan DA, Kann BH, Aerts JWJ, Mak RH. *Nat Rev Clin Oncol.* 2020; 17: 771–781. DOI: 10.1038/s41571-020-0417-8 [PubMed: 32843739]
- [172]. Draguet C, Barragán-Montero AM, Vera MC, Thomas M, Populaire P, Defraene G, Haustermans K, Lee JA, Sterpin E. *Radiother Oncol.* 2022; 176: 101–107. DOI: 10.1016/j.radonc.2022.08.031 [PubMed: 36167194]
- [173]. Saxena S, Jena B, Gupta N, Das S, Sarmah D, Bhattacharya P, Nath T, Paul S, Fouda MM, Kalra M, Saba L, et al. *Cancers (Basel).* 2022; 14: 2860. doi: 10.3390/cancers14122860 [PubMed: 35740526]
- [174]. Guiot J, Vaidyanathan A, Deprez L, Zerka F, Danthine D, Frix A, Lambin P, Bottari F, Tsoutzidis N, Miraglio B, Walsh S, et al. *Med Res Rev.* 2022; 42: 426–440. DOI: 10.1002/med.21846 [PubMed: 34309893]

- [175]. Primakov SP, Ibrahim A, van Timmeren JE, Wu G, Keek SA, Beuque M, Granzier RWY, Lavrova E, Scrivener M, Sanduleanu S, Kayan E, et al. *Nature Commun.* 2022; 13: 3423. doi: 10.1038/s41467-022-30841-3 [PubMed: 35701415]
- [176]. Isensee F, Jaeger PF, Kohl SAA, Petersen J, Maier-Hein KH. *Nat Methods.* 2021; 18: 203–211. DOI: 10.1038/s41592-020-01008-z [PubMed: 33288961]
- [177]. McIntosh C, Conroy L, Tjong MC, Craig T, Bayley A, Catton C, Gospodarowicz M, Helou J, Isfahanian N, Kong V, Lam T, et al. *Nature Med.* 2021; 27: 999–1005. DOI: 10.1038/s41591-021-01359-w [PubMed: 34083812]
- [178]. van den Berg CAT, Melià EF. *Semin Radiat Oncol.* 2022; 32: 304–318. DOI: 10.1016/j.semradonc.2022.06.001 [PubMed: 36202434]
- [179]. Zhao W, Shen L, Islam MT, Qin W, Zhang Z, Liang X, Zhang G, Xu S, Li X. *Quant Imaging Med Surg.* 2021; 11: 4881–4894. DOI: 10.21037/qims-21-199 [PubMed: 34888196]
- [180]. Howard FM, Kochanny S, Koshy M, Spiotto M, Pearson AT. *JAMA Netw Open.* 2020; 3 e2025881 doi: 10.1001/jamanetworkopen.2020.25881 [PubMed: 33211108]
- [181]. Hu Z, Li G, Zhang X, Ye K, Lu J, Peng H. *Phys Med Biol.* 2020; 65 185003 doi: 10.1088/1361-6560/ab9707 [PubMed: 32460246]
- [182]. Rahman AU, Nemallapudi MV, Chou C-Y, Lin C-H, Lee S-C. *Phys Med Biol.* 2022; 67 185010 doi: 10.1088/1361-6560/ac8af5
- [183]. Liu C-C, Huang H-M. *Phys Med Biol.* 2020; 69: 110–119. DOI: 10.1016/j.ejmp.2019.12.006
- [184]. Polf JC, Barajas CA, Peterson SW, Mackin DS, Beddar S, Ren L, Gobbert MK. *Front Phys.* 2022; 10 doi: 10.3389/fphy.2022.838273
- [185]. Jiang Z, Sun L, Yao W, Wu QJ, Xiang L, Ren L. *Phys Med Biol.* 2022; 67 215012 doi: 10.1088/1361-6560/ac9881
- [186]. Yabe T, Yamamoto S, Oda M, Mori K, Toshito T, Akagi T. *Med Phys.* 2020; 47: 3882–3891. DOI: 10.1002/mp.14372 [PubMed: 32623747]
- [187]. Kurz C, Maspero M, Savenije MHF, Landry G, Kamp F, Pinto M, Li M, Parodi K, Belka C, van den Berg CAT. *Phys Med Biol.* 2019; 64 225004 doi: 10.1088/1361-6560/ab4d8c [PubMed: 31610527]
- [188]. Thummerer A, Seller Oria C, Zaffino P, Meijers A, Guterres Marmitt G, Wijsman R, Seco J, Langendijk JA, Knopf A, Spadea MF, Both S. *Med Phys.* 2021; 48: 7673–7684. DOI: 10.1002/mp.15333 [PubMed: 34725829]
- [189]. Thummerer A, Seller Oria C, Zaffino P, Visser S, Meijers A, Guterres Marmitt G, Wijsman R, Seco J, Langendijk JA, Knopf AC, Spadea MF, et al. *Med Phys.* 2022; 49: 6824–6839. DOI: 10.1002/mp.15930 [PubMed: 35982630]
- [190]. Pastor-Serrano O, Perkó Z. *Phys Med Biol.* 2022; 67 105006 doi: 10.1088/1361-6560/ac692e
- [191]. Zhang X, Hu Z, Zhang G, Zhuang Y, Wang Y, Peng H. *Med Phys.* 2021; 48: 2646–2660. DOI: 10.1002/mp.14781 [PubMed: 33594673]
- [192]. Brock KK. *Semin Radiat Oncol.* 2019; 29: 181–184. DOI: 10.1016/j.semradonc.2019.02.011 [PubMed: 31027635]
- [193]. Glide-Hurst CK, Lee P, Yock AD, Olsen JR, Cao M, Siddiqui F, Parker W, Doemer A, Rong Y, Kishan AU, Benedict SH, et al. *Int J Radiat Oncol.* 2021; 109: 1054–1075. DOI: 10.1016/j.ijrobp.2020.10.021
- [194]. Paganetti H, Botas P, Sharp GC, Winey B. *Phys Med Biol.* 2021; 66 22TR01 doi: 10.1088/1361-6560/ac344f
- [195]. Chang C-W, Zhou S, Gao Y, Lin L, Liu T, Bradley JD, Zhang T, Zhou J, Yang X. *Phys Med Biol.* 2022; 67 215004 doi: 10.1088/1361-6560/ac9663
- [196]. Zhang G, Chen X, Dai J, Men K. *Phys Med Biol.* 2022; 103: 18–25. DOI: 10.1016/j.ejmp.2022.09.018
- [197]. Zhang G, Zhou L, Han Z, Zhao W, Peng H. *Phys Med Biol.* 2022; 67 245010 doi: 10.1088/1361-6560/aca517
- [198]. Favaudon V, Caplier L, Monceau V, Pouzoulet F, Sayarath M, Fouillade C, Poupon M, Brito I, Hupé P, Bourhis J, Hall J, et al. *Sci Transl Med.* 2014; 6 245ra93 doi: 10.1126/scitranslmed.3008973

- [199]. Montay-Gruel P, Bouchet A, Jaccard M, Patin D, Serduc R, Aim W, Petersson K, Petit B, Bailat C, Bourhis J, Bräuer-Krisch E, et al. *Radiother Oncol.* 2018; 129: 582–588. DOI: 10.1016/j.radonc.2018.08.016 [PubMed: 30177374]
- [200]. Gao F, Yang Y, Zhu H, Wang J, Xiao D, Zhou Z, Dai T, Zhang Y, Feng G, Li J, Lin B, et al. *Radiother Oncol.* 2022; 166: 44–50. DOI: 10.1016/j.radonc.2021.11.004 [PubMed: 34774651]
- [201]. Diffenderfer ES, Sørensen BS, Mazal A, Carlson DJ. *Med Phys.* 2022; 49: 2039–2054. DOI: 10.1002/mp.15276 [PubMed: 34644403]
- [202]. Tessonier T, Mein S, Walsh DWM, Schuhmacher N, Liew H, Cee R, Galonska M, Scheloske S, Schömers C, Weber U, Brons S, et al. *Int J Radiat Oncol.* 2021; 111: 1011–1022. DOI: 10.1016/j.ijrobp.2021.07.1703
- [203]. Tinganelli W, Weber U, Puspitasari A, Simoniello P, Abdollahi A, Oppermann J, Schuy C, Horst F, Helm A, Fournier C, Durante M. *Radiother Oncol.* 2022; 175: 185–190. DOI: 10.1016/j.radonc.2022.05.003 [PubMed: 35537606]
- [204]. Gaide O, Herrera F, Jeanneret Sozzi W, Gonçalves Jorge P, Kinj R, Bailat C, Duclos F, Bochud F, Germond J-F, Gondré M, Boelhen T, et al. *Radiother Oncol.* 2022; 174: 87–91. DOI: 10.1016/j.radonc.2021.12.045 [PubMed: 34998899]
- [205]. Mascia AE, Daugherty EC, Zhang Y, Lee E, Xiao Z, Sertorio M, Woo J, Backus LR, McDonald JM, McCann C, Russell K, et al. *JAMA Oncol.* 2022; doi: 10.1001/jamaoncol.2022.5843
- [206]. Zelefsky MJ, Yamada Y, Greco C, Lis E, Schöder H, Lobaugh S, Zhang Z, Braunstein S, Bilsky MH, Powell SN, Kolesnick R, et al. *Int J Radiat Oncol.* 2021; 110: 672–679. DOI: 10.1016/j.ijrobp.2021.01.004
- [207]. El Naqa I, Pogue BW, Zhang R, Oraiqat I, Parodi K. *Med Phys.* 2022; 49: 4109–4122. DOI: 10.1002/mp.15662 [PubMed: 35396707]
- [208]. Weber UA, Scifoni E, Durante M. *Med Phys.* 2022; 49: 1974–1992. DOI: 10.1002/mp.15135 [PubMed: 34318508]
- [209]. Jolly S, Owen H, Schippers M, Welsch C. *Phys Medica.* 2020; 78: 71–82. DOI: 10.1016/j.ejmp.2020.08.005
- [210]. Simeonov Y, Weber U, Schuy C, Engenhardt-Cabillic R, Penchev P, Durante M, Zink K. *Z Med Phys.* 2021; 31: 203–214. DOI: 10.1016/j.zemedi.2020.06.008 [PubMed: 32711939]
- [211]. Simeonov Y, Weber U, Penchev P, Ringbæk TP, Schuy C, Brons S, Engenhardt-Cabillic R, Bliedtner J, Zink K. *Phys Med Biol.* 2017; 62: 7075–7096. DOI: 10.1088/1361-6560/aa81f4 [PubMed: 28741595]
- [212]. Simeonov Y, Weber U, Schuy C, Engenhardt-Cabillic R, Penchev P, Flatten V, Zink K. *Biomed Phys Eng Express.* 2022; 8 035006 doi: 10.1088/2057-1976/ac5937
- [213]. Tommasino F, Rovituro M, Bortoli E, La Tessa C, Petringa G, Lorentini S, Verroi E, Simeonov Y, Weber U, Cirrone P, Schwarz M, et al. *Phys Medica.* 2019; 58: 99–106. DOI: 10.1016/j.ejmp.2019.02.001
- [214]. Luoni F, Weber U, Boscolo D, Durante M, Reidel C-A, Schuy C, Zink K, Horst F. *Front Phys.* 2020; 8 doi: 10.3389/fphy.2020.568145
- [215]. Kang M, Wei S, Choi JI, Lin H, Simone CB. *Int J Radiat Oncol.* 2022; 113: 203–213. DOI: 10.1016/j.ijrobp.2022.01.009
- [216]. MacKay R, Burnet N, Lowe M, Rothwell B, Kirkby N, Kirkby K, Hendry J. *Radiother Oncol.* 2021; 164: 122–127. DOI: 10.1016/j.radonc.2021.09.011 [PubMed: 34563608]
- [217]. Schwarz M, Traneus E, Safai S, Kolano A, Water S. *Med Phys.* 2022; 49: 2861–2874. DOI: 10.1002/mp.15579 [PubMed: 35213040]
- [218]. Ramesh P, Gu W, Ruan D, Sheng K. *Med Phys.* 2022; 49: 7826–7837. DOI: 10.1002/mp.16009 [PubMed: 36222217]
- [219]. Chaudhary P, Milluzzo G, Ahmed H, Odlozilik B, McMurray A, Prise KM, Borghesi M. *Front Phys.* 2021; 9 doi: 10.3389/fphy.2021.624963
- [220]. Chaudhary P, Gwynne DC, Odlozilik B, McMurray A, Milluzzo G, Maiorino C, Doria D, Ahmed H, Romagnani L, Alejo A, Padda H, et al. *Radiat Oncol.* 2022; 17: 77. doi: 10.1186/s13014-022-02024-3 [PubMed: 35428301]

- [221]. Chaudhary P, Milluzzo G, McIlvenny A, Ahmed H, McMurray A, Maiorino C, Polin K, Romagnani L, Doria D, McMahon SJ, Botchway SW, et al. *Phys Med Biol.* 2023; 68 025015 doi: 10.1088/1361-6560/aca387



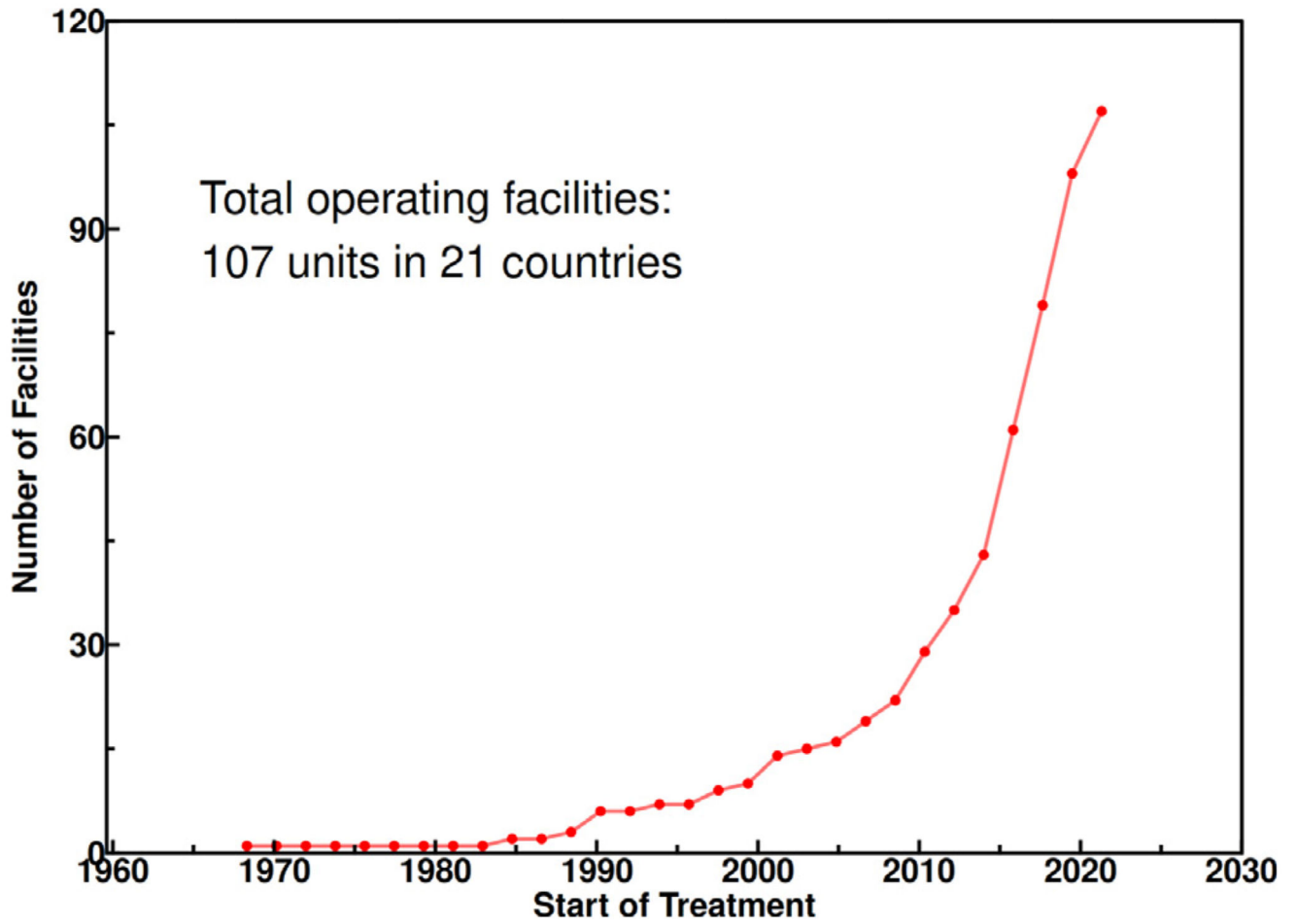


**Fig 1.** The growth of the particle therapy facilities worldwide.  
*Source:* Data from PTCOG [9].

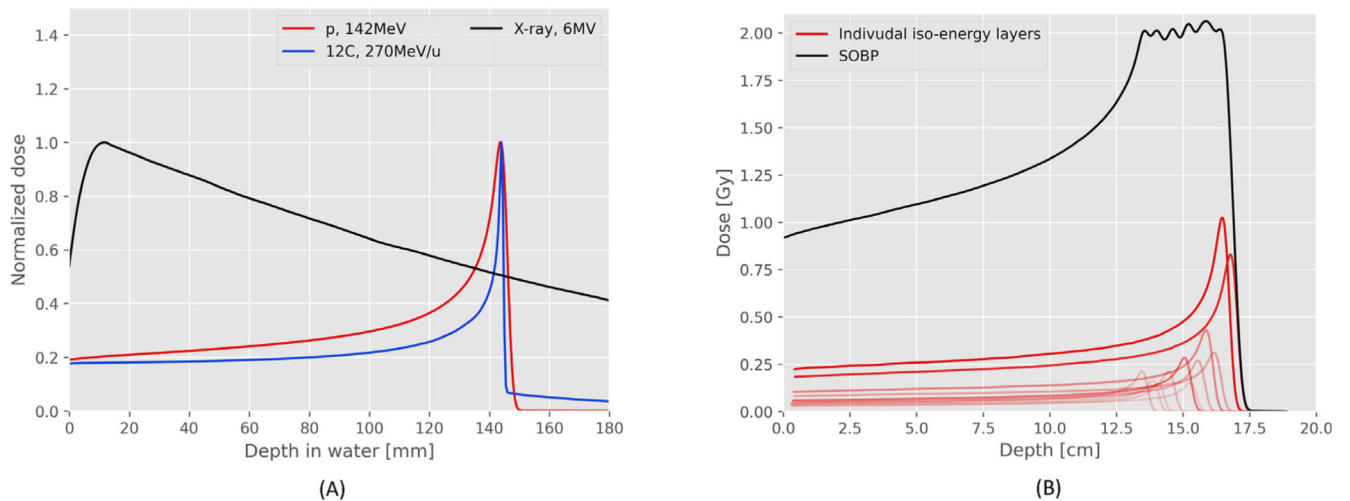


**Fig 2. Physical advantages of charged particle therapy.**

A, depth-dose distributions of high-energy X-rays and monoenergetic beams of protons or carbon ions. At the same range, C-ions have lower straggling than protons, but a tail of fragments is visible beyond the Bragg peak. The curves were generated with TOPAS [34]/Geant4 simulations. In clinical applications, the Bragg peak must be extended to cover the whole tumor (Spread-Out-Bragg-Peak, SOBP) (B). This can be done by overlapping different pristine beams at different energy and intensity, as shown for protons.

*Source:* Data generated with TRiP98 [35].

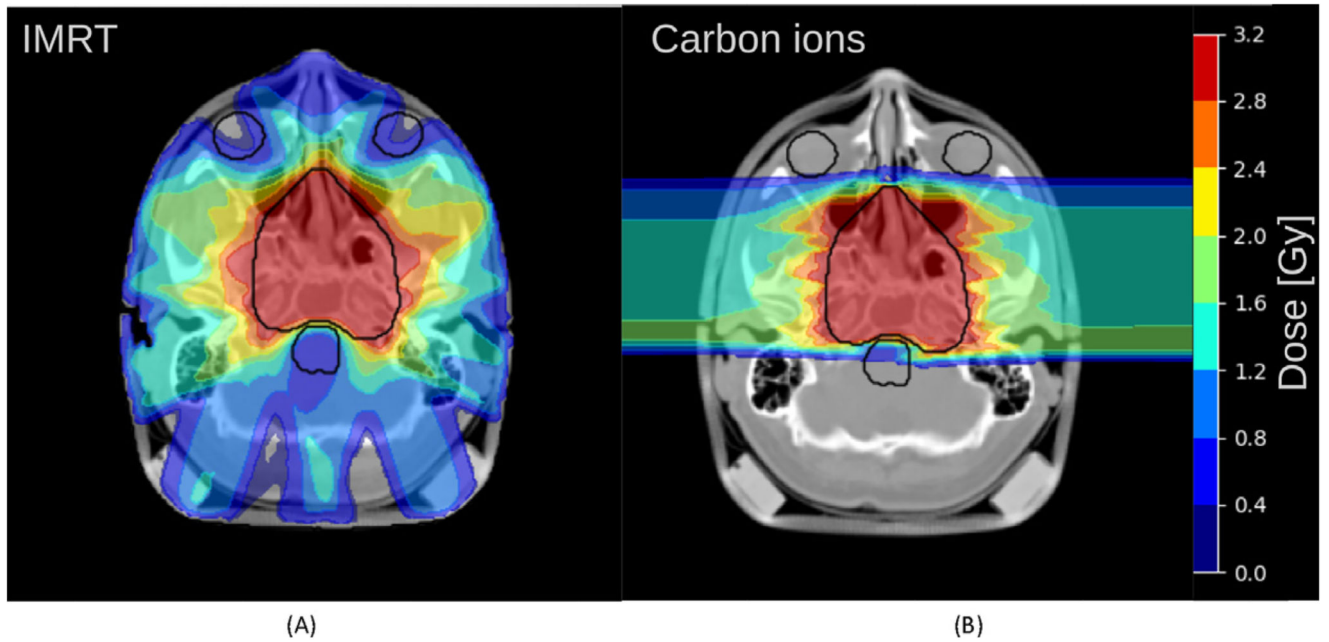


**Fig 3.** Comparison of treatment plans for a chordoma patient with a large central tumor for A. IMRT (9 fields) or B. carbon ions (2 fields). The IMRT plan was generated with the MatRad [36] open treatment planning toolkit, the carbon plan was generated with TRiP98 [35]. The substantial reduction in the integral dose to the normal tissue and the sparing of critical structures is clear using particles.

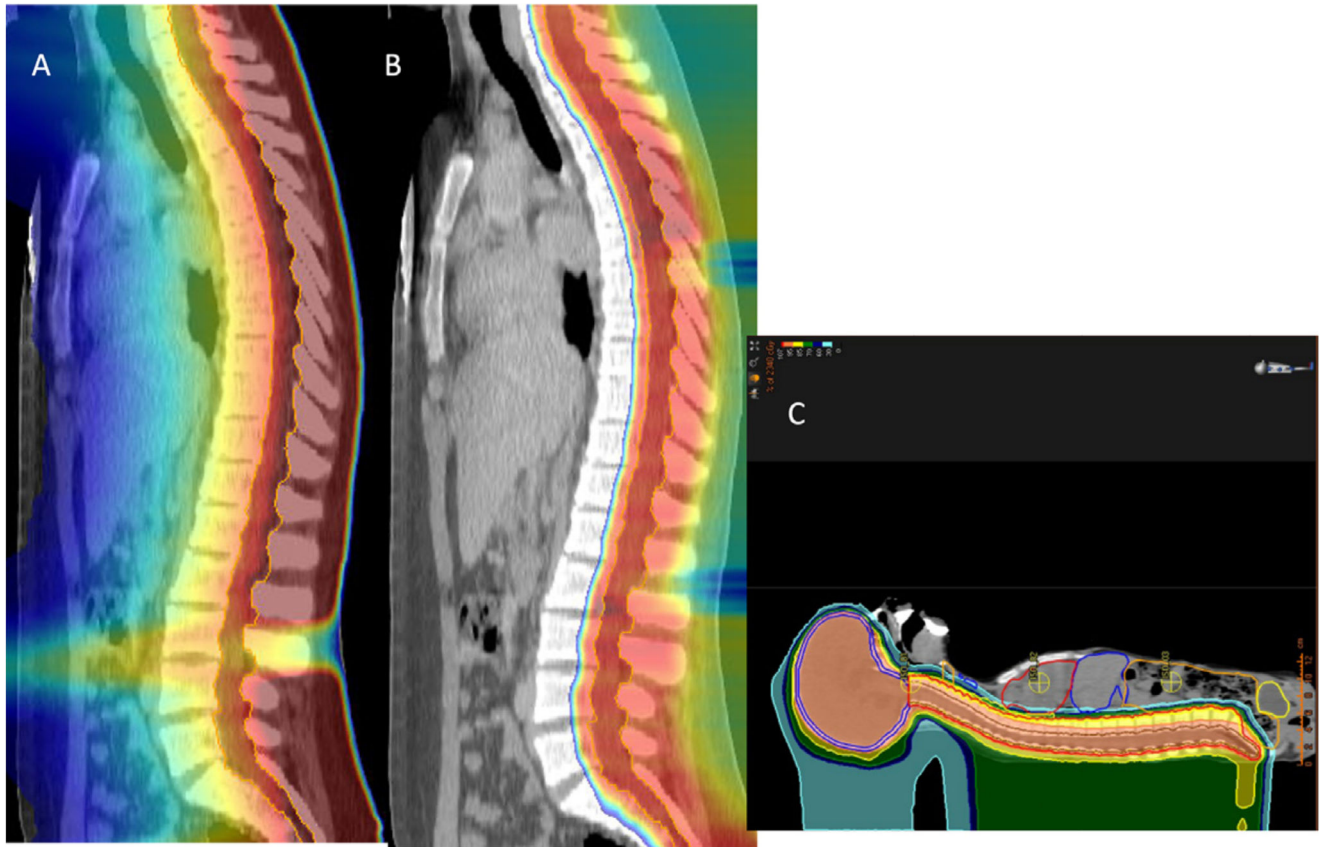


**Fig 4. Craniospinal irradiation of a pediatric medulloblastoma patient.**

A. IMRT plan, B. proton plan. C. full proton plan including the brain and the countering of the internal organs at risk.

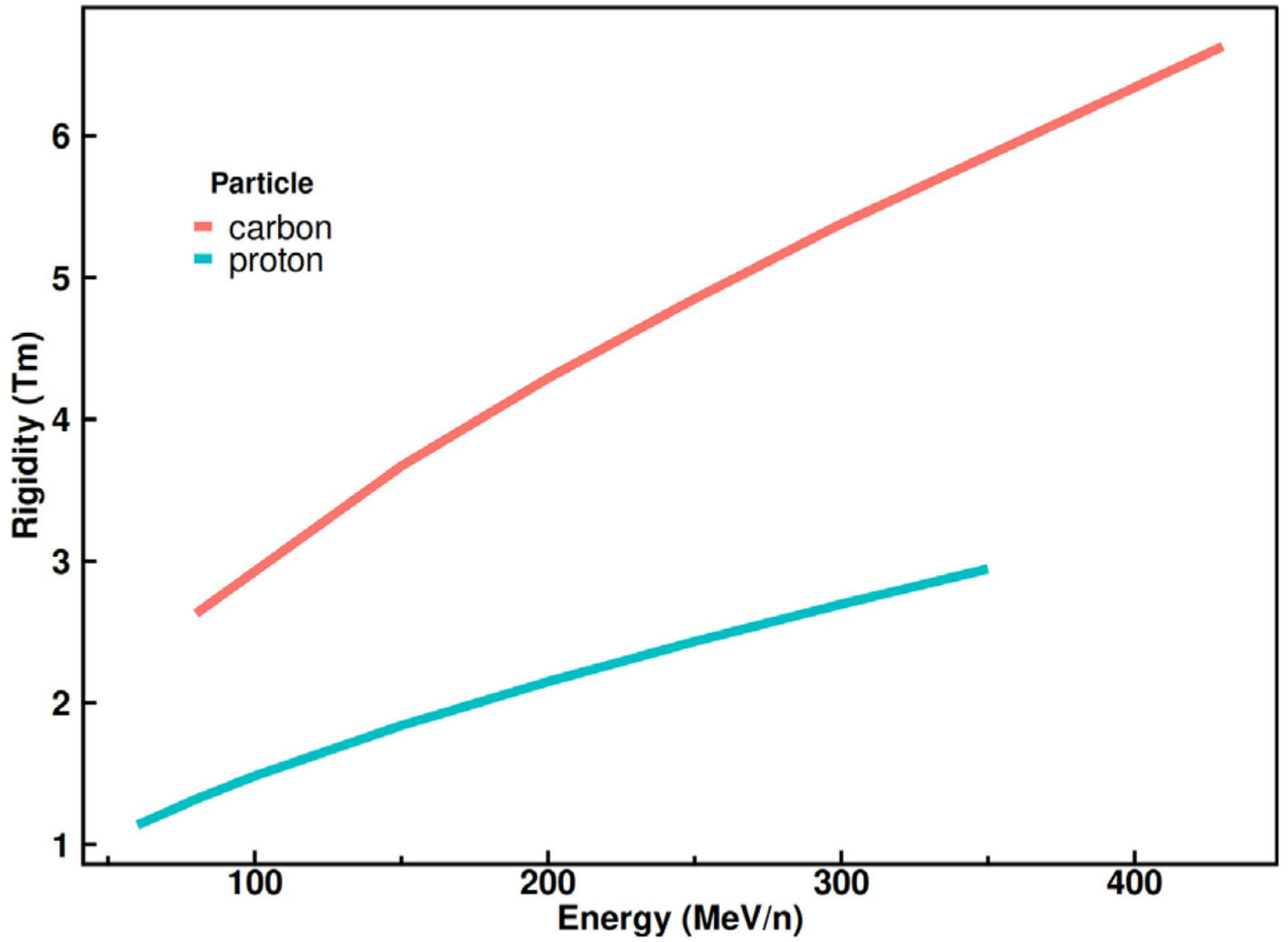
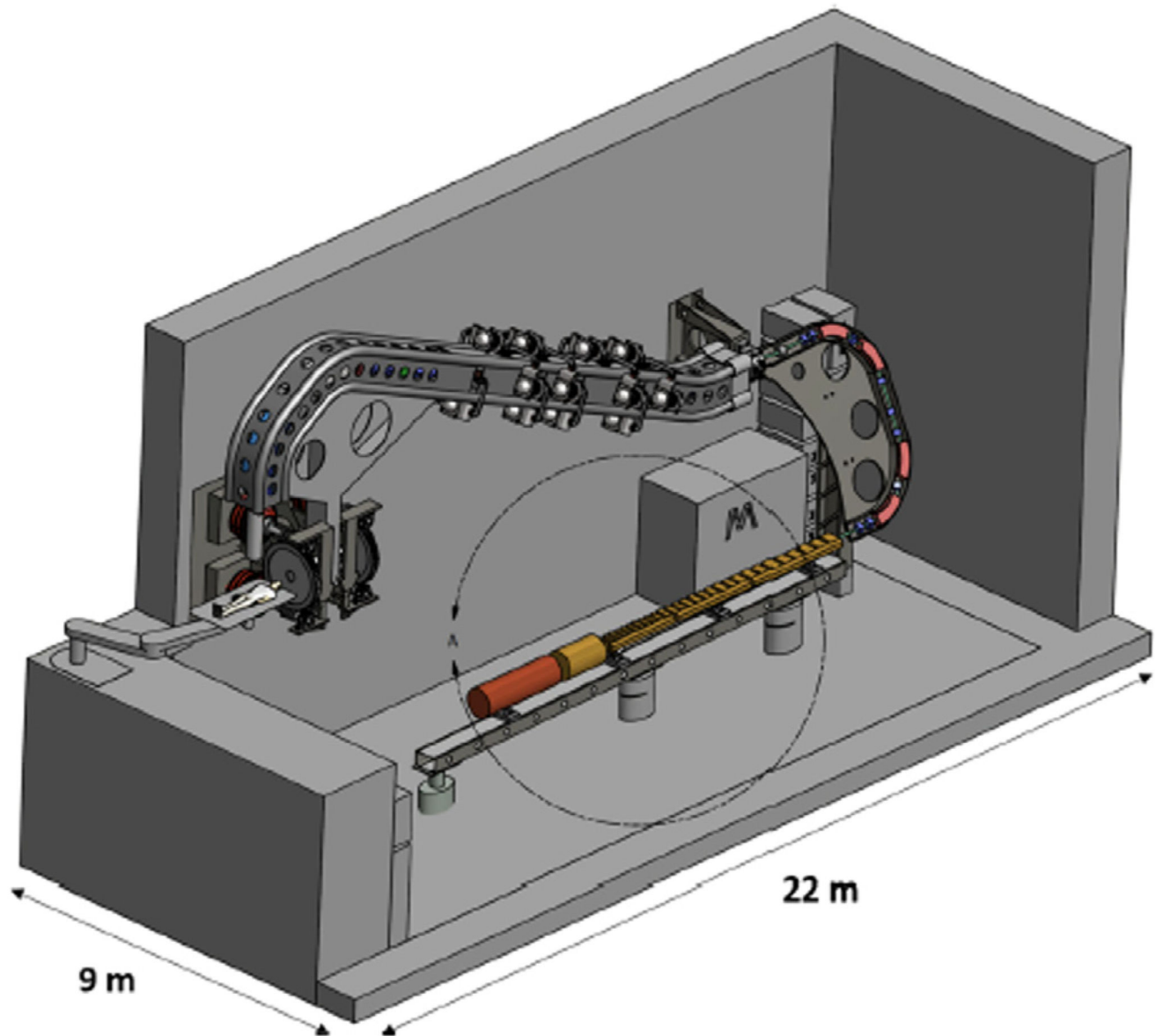
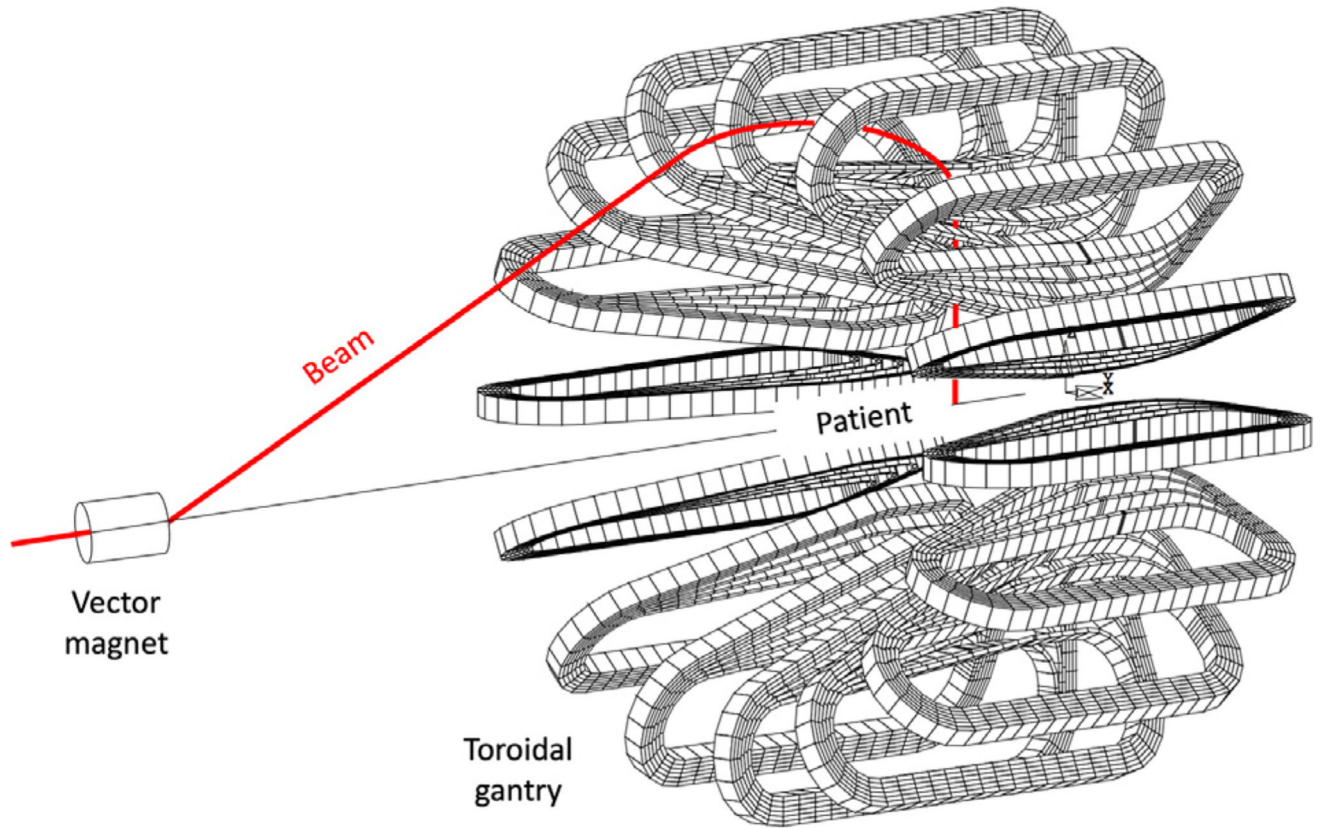


Fig 5. Magnetic rigidity as a function of the particle energy for protons and carbon ions.



**Fig 6. Sketch of the TULIP all-linac accelerator.**

*Source:* Image from Ref. [58], reproduced with permission.



**Fig 7. Sketch of a toroidal fixed gantry, with 16 superconducting coils, able to deliver the beam from any angle without rotation.**

*Source:* Image from Ref. [75], reproduced with permission.

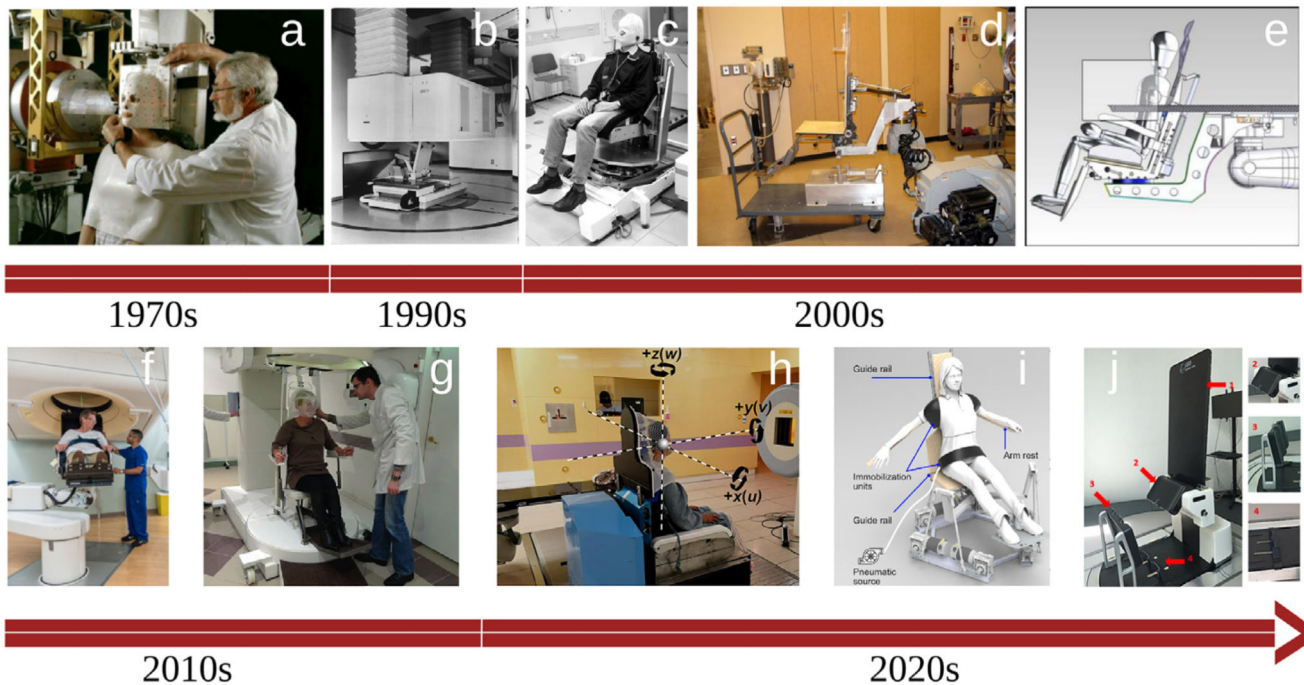


**Fig 8. Historical overview over different upright positioning systems used for particle therapy.** a upright positioner for the pioneering studies at Lawrence Berkeley National Lab (Source: imaging archive of the Lawrence Berkeley National Laboratory, © 2010–2019 The Regents of the University of California, Lawrence Berkeley National Laboratory). b Chair positioner and vertical CT scanner at the Hyogo HIMAC, Japan [76]. c Chair prototype at the GSI carbon ion therapy pilot project [77]. d and e Chair positioners used at the Indiana University Health Proton Therapy Center and the Oklahoma Proton Center, respectively [78]. f Chair system in operation at Northwestern Medicine Chicago Proton Center. Image courtesy to Northwestern Medicine Chicago Proton Center. g Chair system of the ‘PROMETHEUS’ proton therapy center at P.N. Lebedev Physical Institute of the Russian Academy of Sciences (Protvino, Russia) [79]. h Chair system at the Shanghai Proton and Heavy Ion Center (Shanghai, China) [80]. i Chair design with soft-robotics immobilization [81]. j Leo Cancer Care upright positioner [82].



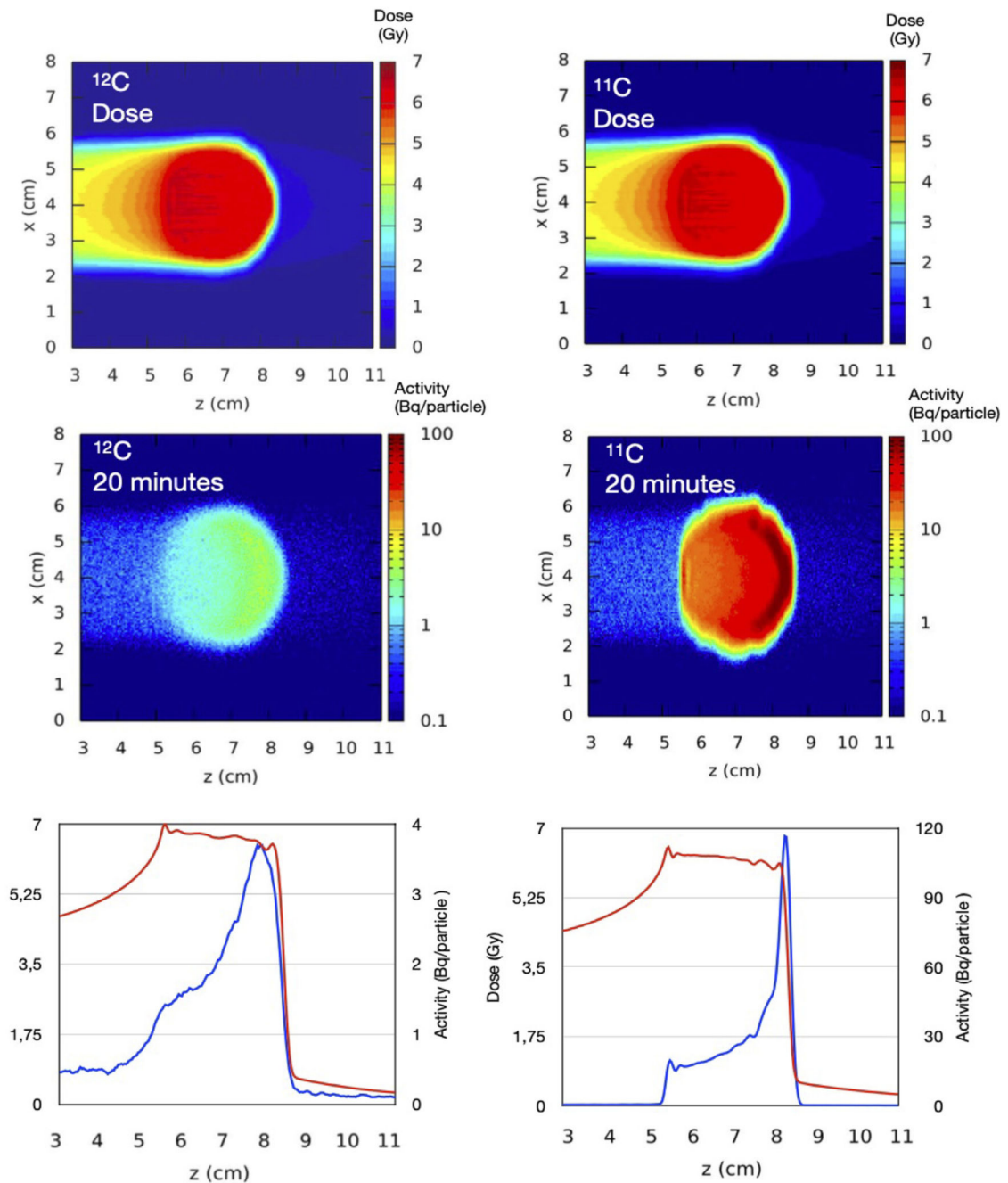


**Fig 9. Potential advantages radioactive ion beams for image-guided radiotherapy.**

The images show Monte Carlo simulation of  $^{12}\text{C}$  and  $^{11}\text{C}$  beams stopping in a spherical water volume and visualized by PET in 20 min. The graphs show the dose (red curve) and the activity (blue curve) distribution along the beam direction (z-axis) showing the shift between dose and activity when stable ions are used. Simulation by Monte Carlo code FLUKA.

*Source:* Image from Ref. [155], reproduced with permission.

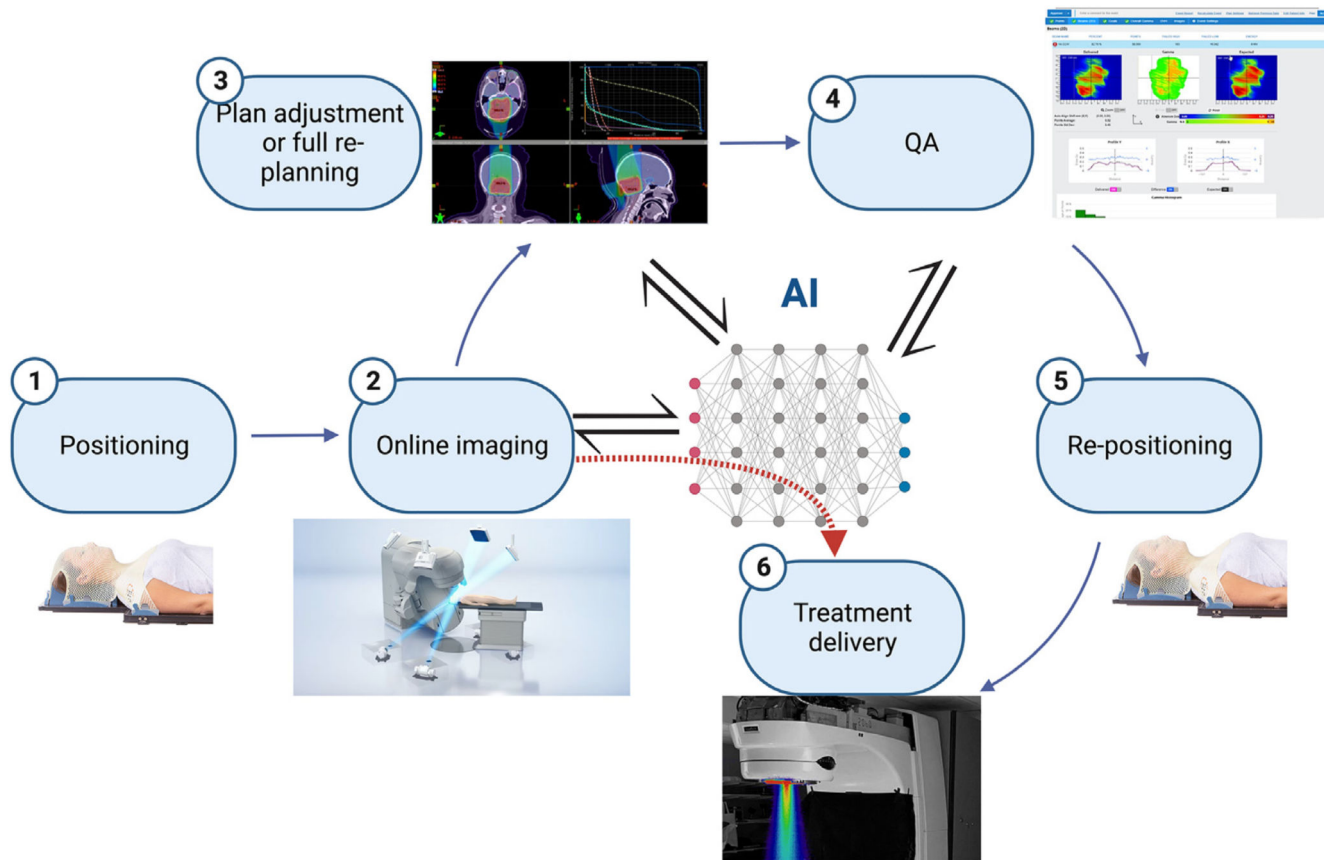


**Fig 10. Potential contribution of AI (here represented as a neural network in the center of the figure) to online adaptive particle therapy.**

The green dashed line corresponds to the possibility to use AI for online beam delivery adaptation to intra-fractional target motion.

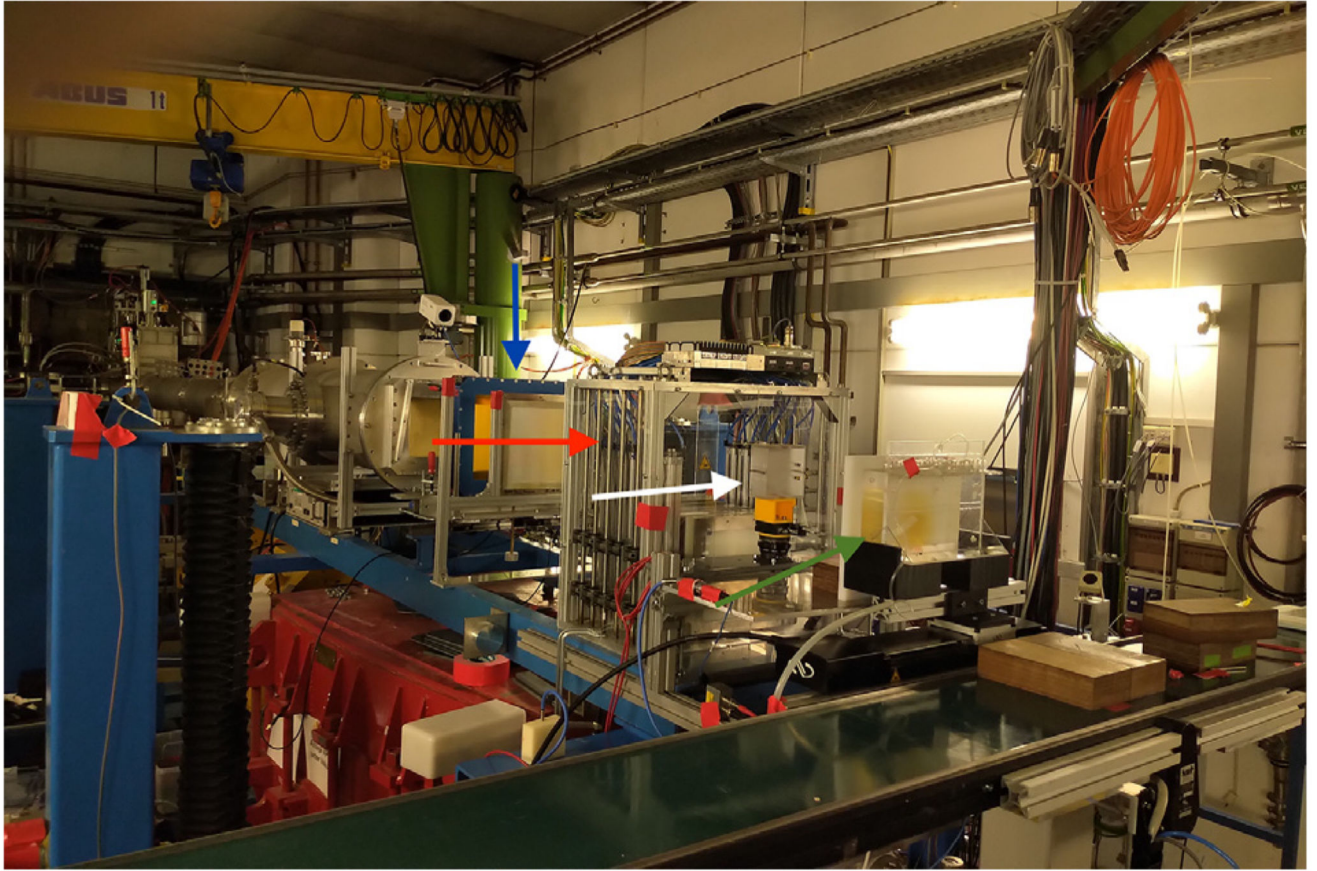


**Fig 11. Beamline for FLASH experiments using carbon ions in the GSI cave A (Darmstadt, Germany).**  
Blu arrow: He/CO<sub>2</sub> filled ionization chamber (beam monitor); red arrow: binary range shifter; white arrow: 3D-printed SOBPs-modulator; green arrow: target station for animal irradiation.

**Table 1**  
**Characteristics of the main accelerators potentially used in particle therapy.**

In parenthesis are the objectives that are planned but not yet reached.

Accelerator	Average size (m)	Energy modulation	Repetition rate (Hz)	Energy range (MeV/n)	Ion species	In use today
Linacs	50	Modules on/off	~200	<20 (200)	1 (2)	Yes
Cyclotrons	5	Absorbers	~10 <sup>6</sup>	70–250	1	Yes
Superconducting cyclotrons	1.5 <sup>b</sup>	Absorbers	~10 <sup>6</sup>	70–250 (400)	1 (multiple)	Yes
Synchrotrons	20	Ramp	0.5–1	70–430	Multiple	Yes
RCMS <sup>c</sup>	20	Ramp	30	70–430	Multiple	No
Cyclinacs	30	Modules on/off	300	70 (430)	2	No
FFAG <sup>d</sup>	18	Ramp	1000	(70–430)	Multiple	No
DWA <sup>e</sup>	2	Modules on/off	50	(200)	1 (2)	No
LDPA <sup>f</sup>	2–3	Selection from full spectrum	≪1 (10)	100 (400)	Multiple	No

<sup>a</sup>Superconducting.

<sup>b</sup>Approximately 6.3 m diameter for the C-ions prototype C400.

<sup>c</sup>Rapid cycling medical synchrotron.

<sup>d</sup>Fixed field alternating gradient.

<sup>e</sup>Dielectric wall accelerator.

<sup>f</sup>Laser-driven particle accelerators.

**Table 2**  
**Characteristics of the main accelerators currently in use for particle therapy.**

Name	Company	Accelerator type	Particle (max energy)	Diameter (m)	Magnet type	Max field (T)
C230	IBA	Isochronous cyclotron	p (230 MeV)	4.3	Normal conducting	1.7
S2C2	IBA	Synchrocyclotron	p (250 MeV)	2.2	Superconducting (NbTi)	5.7
Probeam	Varian	Isochronous cyclotron	p (250 MeV)	3.1	Superconducting (NbTi)	2.4
SC360	ProNova	Isochronous cyclotron	p (250 MeV)	2.8	Superconducting (NbTi)	4
SC230	Sumitomo	Isochronous cyclotron	P (230 MeV)	2.8	Superconducting (NbTi)	4
S250	Mevion	Synchrocyclotron	p (250 MeV)	1.5	Superconducting (Nb <sub>3</sub> Sn)	9
PROBEAT	Hitachi	Synchrotron	p (220 MeV)	5.1	Normal conducting	1.8
Conforma 3000	Optivus	Synchrotron	P (250 MeV)	8	Normal conducting	1.4
Radiance	ProTom	Synchrotron	p (330 MeV)	4.1	Normal conducting	1.9
Toshiba	Toshiba	Synchrotron	C (430 MeV/n)	20	Normal conducting	1.5
PIMMS	CERN	Synchrotron	C (400 MeV/n)	25	Normal conducting	1.5
PTS	SIEMENS	Synchrotron	C (430 MeV/n)	20	Normal conducting	1.43
HITACHI	Hitachi	Synchrotron	C (430 MeV/n)	17	Normal conducting	1.5
C400	IBA	Isochronous cyclotron	C (400 MeV/n)	6.6	Superconducting	4.5

**Table 3**  
**Estimated proton range uncertainties, their sources, and the potential of Monte Carlo for reducing the uncertainty.**

*Source:* Table modified from ref. [15,40].

Source of uncertainty	Uncertainty type	Range uncertainty
Commissioning	Measurement uncertainty in water	$\pm 0.3$ mm
Beam delivery	Compensator design	$\pm 0.2$ mm
	Beam reproducibility	$\pm 0.2$ mm
Positioning	Patient setup	$\pm 0.7$ mm
Biology	Biological range extension	$\approx 0.8\%$ (always positive)
Dose calculation	CT imaging and calibration	$\pm 0.5\%$
	CT conversion to tissue	$\pm 0.5\%$
	CT grid size	$\pm 0.3\%$
	Mean excitation value (I-value) in tissue	$\pm 1.5\%$
	Range degradation	$\pm 2.5\%$
Total (excluding biology)		4.6% + 1.2 mm
Total (using Monte Carlo dose calculation)		2.4% + 1.2 mm